https://doi.org/10.5194/egusphere-2026-6556
Preprint. Discussion started: 16 November 2026
© Author(s) 2026. CC BY 4.0 License.

Measurement Report: PM10-Bound Organic Molecular Tracers (Saccharides) from an Agro-Industrial Metropolis in the Indo-Gangetic Plain (IGP): Seasonal Variations and Source Attribution

Muhammad Usman Alvi[1*]. Junaid Anwer[1]. Farhan Anwer[2]

1 Department of Chemistry, University of Okara, Okara, 56300, Pakistan
2 Department of Physics, University of Okara, Okara, 56300, Pakistan

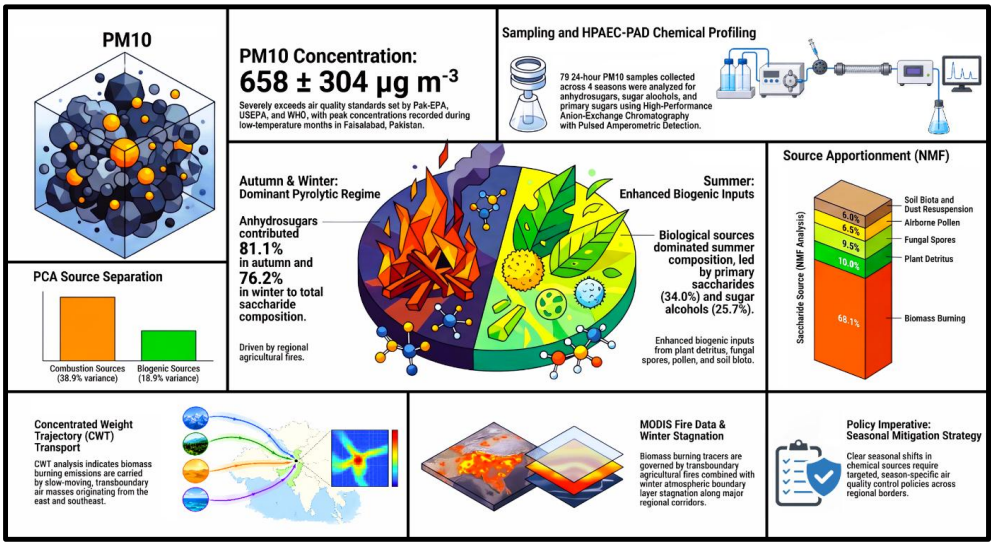
***Corresponding author:**
Muhammad Usman Alvi[1*] (usm_alvi@hotmail.com)
1 Department of Chemistry, University of Okara, Okara, 56300, Pakistan

Abstract

The Indo Gangetic Plain (IGP) is facing serious environmental and public health challenges due to severe particulate matter (PM10) pollution, aggravated by smog and agricultural burning. In this study, airborne saccharides are characterized from Faisalabad, Pakistan throughout four different seasons. Seventy-nine 24-hour (PM10) samples were analyzed for saccharides including anhydrosugars, sugar alcohols, and primary sugars by HPAEC-PAD. The average PM10 value was 658 ± 304 µg m^{-3}, exceeding the safety limits by Pak-EPA, USEPA, and WHO. The highest concentrations were observed during low temperature months. During Autumn and Winter, the pyrolytic regime was dominant due to regional agricultural fires, having highest contributions from anhydrosugars (81.1 % and 76.2 %, respectively). In contrast, summer samples showed an enhanced input from biological sources where primary saccharides and sugar alcohols gave the highest relative contribution (34.0 % and 25.7 %, respectively). CWT analysis showed that biomass burning emissions were transported by slow moving, transboundary air masses from the east and southeast. PCA isolated combustion sources (38.9 % variance) from that of biogenic sources (18.9 % variance). NMF analysis identified five saccharide sources: biomass burning (68.1 %), plant detritus (10.0 %), fungal spores (9.5 %), airborne pollen (6.5 %) and soil biota and dust resuspension (6.0 %). MODIS fire data revealed that biomass burning tracers are mainly controlled by transboundary agricultural burning and winter boundary layer stagnation along the main regional air corridors. The results show a clear seasonal separation and necessitate the seasonal air quality mitigating measures in the region.

Keywords: Airborne Particulate Matter; Principal Component Analysis; Levoglucosan; Biomass Burning; Non-Negative Matrix Factorization

https://doi.org/10.5194/egusphere-2026-6556
Preprint. Discussion started: 16 November 2026
© Author(s) 2026. CC BY 4.0 License.



Graphical Abstract

https://doi.org/10.5194/egusphere-2026-6556
Preprint. Discussion started: 16 November 2026
© Author(s) 2026. CC BY 4.0 License.

1. Introduction

Airborne particulate matter (PM) is a mixture of solid and liquid particles that are complex in nature and has a significant role in the Earth's radiative balance and regional climate dynamics (Adam et al., 2021; Vincenti et al., 2022). PM10 (particles with an aerodynamic diameter ≤10 μm) is a vital air quality indicator since it can be suspended for extended periods and propagate over great distances (Valavanidis et al., 2008; Islam et al., 2020). These particles affect climate directly through reflecting and absorbing solar energy and indirectly as cloud condensation nuclei (CCN) and hence influence cloud albedo and precipitation patterns (Andreae and Rosenfeld, 2008; Theodosi et al., 2018; Fu et al., 2024). In addition to environmental effects, exposure to PM10 is a serious public health hazard. These particles are small enough to penetrate deep into the human respiratory and circulatory systems, causing asthma, bronchitis, rhinitis, pneumonia, chronic obstructive pulmonary disease (COPD), lung cancer, hypertension, myocardial infarction, cardiac arrhythmias, stroke, renal failure, disruption of the endocrine system, infertility, and pre-mature infant deaths (Pope and Dockery, 2006; Kampa and Castanas, 2008; Valavanidis et al., 2008; Burnett et al., 2018; Manojkumar and Srimuruganandam, 2021; Pardo et al., 2022; Ramteke et al., 2022; Ramteke et al., 2025; Kolawole et al., 2026). Fine particulate matter is considered as the fourth leading cause of deaths worldwide, causing 8 % of all global deaths. According to the World Health Organization (WHO), the vast majority of the 4.2 million global air pollution deaths in 2016 occurred in low to middle income countries within South Asia, East Asia, and the Western Pacific (Islam et al., 2020, 2022).

South Asia in general and Indo-Gangetic Plain (IGP) in particular has emerged as one of the most polluted and crowded regions of the world (Bhattarai et al., 2019; Saikawa et al., 2019). This region including Pakistan, India, Nepal and Bangladesh has often PM levels many times higher than the air quality limits of the WHO. In 2016, the WHO listed several major Pakistani cities, including Lahore, Rawalpindi, Karachi, and Peshawar, among the top

https://doi.org/10.5194/egusphere-2026-6556
Preprint. Discussion started: 16 November 2026
© Author(s) 2026. CC BY 4.0 License.

50 most polluted cities worldwide. The topographical vulnerability of this region is also attributed to its proximity to the Himalayas (Islam et al., 2020, 2021). Reports by the Pakistan Environmental Protection Agency (Pak-EPA), the World Bank, and the Economic Survey of Pakistan, identify high particulate matter concentrations, expanding industrial operations, and rapid vehicular growth as key drivers of ambient air degradation (Gheorghe and Ion, 2011; Adrees et al., 2016). To manage air pollution, the Pakistani government established the Pakistan Clean Air Program (PCAP) and drafted National Environmental Quality Standards (NEQS) for industrial emissions in 1997 and vehicular emissions in 1999. Although these standards were later reviewed by Pak-EPA, assessments by the World Bank highlight that current NEQS thresholds remain outdated and exceed WHO safety guidelines and United States Environment Protection Agency (USEPA) National Ambient Air Quality Standards (NAAQS) (Table 1). While PCAP outlined short and long term control strategies, no substantial actions have been executed.

One of the major issues for the IGP is the frequent severe smog and haze events throughout the post-cultivation and winter seasons (Rajput et al., 2011; Fu et al., 2024). Large scale post-harvest burning of crop residues (e.g. rice and wheat straw) between October and November generates large volumes of carbonaceous aerosols (Bhattarai et al., 2019; Fu et al., 2024). These emissions, together with the burning of domestic wood and animal dung for heating and cooking, cause recurring spells of smog, with the air visibility often dropping below 1 km during severe peaks (Shahzad et al., 2013). Data from the 7th Population and Housing Census 2023 revealed traditional biomass as the dominant household cooking fuel (56.6 %) across Pakistan. This high reliance is closely tied to the country's demographic distribution, with 61 % of the population living in rural areas. Further, the situation is aggravated by by factors such as “meteorological trapping”, during which the planetary boundary layer (PBL) height decreases dramatically (often below 1000 m or even 100 m),

https://doi.org/10.5194/egusphere-2026-6556
Preprint. Discussion started: 16 November 2026
© Author(s) 2026. CC BY 4.0 License.

Table 1 Summary of the air quality standards established by Pak-EPA, US-EPA and WHO

Pollutants	NEQS by Pak-EPA			NAAQS by US-EPA		WHO	
	Average Time	Concentration 2009	Concentration 2012	Average Time	Concentration	Average Time	Concentration
Sulphur Dioxide (SO_2) µg m^{-3}	24 Hrs[b)]	120	120	24 Hrs	140[d)]	24 Hrs	20
	1 Year[b)]	80	80	1 Year	30[d)]	1 Year	50
Oxides of Nitrogen as (NO) µg m^{-3}	24 Hrs[b)]	40	40	–	–	–	–
	1 Year[b)]	40	40				
Oxides of Nitrogen as (NO_2) µg m^{-3}	24 Hrs[b)]	80	80	1 Year	53[d)]	1 Hr	200
	1 Year[b)]	40	40			1 Year	40
O_3 µg m^{-3}	1 Hr	180	130	1 Hr	120[d)]	8 Hrs	100
				8 Hrs	80[d)]		
Suspended Particulate Matter (SPM) µg m^{-3}	24 Hrs[b)]	550	500	–	–	24 Hrs	120
	1 Year[a)]	400	360				
Respirable Particulate Matter (PM10) µg m^{-3}	24 Hrs[b)]	250	150	24 Hrs	150	24 Hr	50
	1 Year[a)]	200	120	1 Year	50	1 Year	20
Reparable Particulate Matter (PM2.5) µg m^{-3}	1 Hr	25	15	24 Hrs	65	1 Hr	1
	24 Hrs[b)]	40	35			24 Hrs	25
	1 Year[a)]	25	15	1 Year	15	1 Year	10
Lead (Pb) µg m^{-3}	24 Hrs[b)]	2.0	1.5	3 months	1.5	1 Year	0.5
	1 Year[a)]	1.5	1.0				
Carbon Monoxide (CO) mg m^{-3}	8 Hrs[b)]	5.0	5.0	1 Hr	35[c)]	1 Hr	30
	24 Hrs[b)]	10	10	8 Hrs	9[c)]	8 Hrs	10

a) Annual arithmetic mean of minimum 104 measurements in a year taken twice a week 24 hourly at uniform interval, b) 24 hourly/8 hourly values should be met 98 % of the year. 2 % of the time, it may exceed but not on two consecutive days, c) Value in ppm, d) Value in ppb

https://doi.org/10.5194/egusphere-2026-6556
Preprint. Discussion started: 16 November 2026
© Author(s) 2026. CC BY 4.0 License.

stagnant wind speeds, and temperature inversions which prevent vertical mixing of pollutants (Huang et al., 2014).

It is crucial to identify the origins of these aerosols with molecular tracers in order to design appropriate mitigation methods. Saccharides (sugars) are widespread water-soluble organic molecules accounting for 13–26 % of the detected organic mass in continental aerosols (Simoneit et al., 2004; Jia et al., 2010; Wang et al., 2021; Vincenti et al., 2022). These markers are divided into Anhydrosugars, Sugar Alcohols and Primary Sugars. Cellulose and hemicellulose pyrolysis produces anhydrosugars, such as Levoglucosan, Mannosan and Galactosan (Suciu et al., 2019; Ankit et al., 2026). Levoglucosan is the definitive tracer for biomass burning and the Levoglucosan/Mannosan ratio is a reliable molecular proxy to identify either burning of crop residue or combustion of softwood and hardwood (Simoneit et al., 1999; Bhattarai et al., 2019; Vincenti et al., 2022). Similarly, sugar alcohols such as Mannitol and Arabitol are specific tracers of airborne fungal spores are (Bauer et al., 2008; Iinuma et al., 2009). Primary Sugars such as Glucose, Fructose, Sucrose and Trehalose are of biogenic origin, e.g. from pollen, microbes and resuspended soil (Simoneit et al., 2004).

There is a need to characterize airborne sugars in the PM10 fraction, which has a greater proportion of biogenic debris and crustal materials (Ramteke et al., 2022). The study seeks to analyze these unique chemical fingerprints that not only reveal specific pollution sources like crop burning, soil dust, and fungal spores, but also their typical concentrations and seasonal changes in the IGP, will provide insights into the complex interplay between agricultural fires and the biogenic background of the region.

1. Materials and Methods

2.1 Site Description

https://doi.org/10.5194/egusphere-2026-6556
Preprint. Discussion started: 16 November 2026
© Author(s) 2026. CC BY 4.0 License.

Faisalabad is the third largest city in Pakistan, situated in the north-western part of the Indo-Gangetic Plain (31.4191° N, 73.0730° E), at an elevation of 184 m above mean sea level. The population of Faisalabad District was 9.076 million in 2023 with a population density of 1,550 persons per km^2 (Pakistan Bureau of Statistics, 2024). Faisalabad is a major hub of the China Pakistan Economic Corridor (CPEC), situated on an important transit link between Islamabad and the Chinese border with the ports of Karachi and Gwadar. According to the Punjab Revenue Department, Faisalabad has 441 thousand hectors of cultivated land, which produces major commodities including wheat, rice, cotton, sugarcane, fruits, and vegetables (Bureau of Statistics, 2026). Faisalabad contributes 5 % of the national GDP of Pakistan and 21 % of its contribution from the agriculture sector (Punjab Board of Investment and Trade, 2024). There are around 65,590 industrial units functioning in the city and its surrounding areas such as food processing industries (flour, sugar, seed oil, beverages, ghee or clarified butter), textile and fabric manufacturing of silk and cotton, hosiery, fertilizers, chemicals, dyes, paper & pulp, agricultural equipment, engineering works, and railroad repair yards (Alvi et al., 2018). Based on the vehicle registration data of the Excise and Taxation Department Punjab (2024), the mobile fleet of Faisalabad is dominated by two-wheelers (91.34 %), while private passenger vehicles (4.69 %) constitute the second largest category. The remaining 3.97 % consist of commercial, transport and agricultural vehicles.

Air pollution in Faisalabad is worsened by unplanned industrial growth, dusty unpaved road edges, poorly maintained vehicles, inefficient use of energy, ineffective treatment of air emissions, open solid waste incineration (including plastics), and emissions of ozone depleting substances (Waheed et al., 2006). Moreover, economic growth is given priority over environmental regulation in developing countries due to financial constraints and political preferences, which results in weak policy frameworks, inadequate air quality management systems and lack of continuous air monitoring stations in the city (Omanga et al., 2014; Lurie et al., 2019; Ma et al., 2019). Consequently, there is a lack of baseline

https://doi.org/10.5194/egusphere-2026-6556
Preprint. Discussion started: 16 November 2026
© Author(s) 2026. CC BY 4.0 License.

empirical data on air pollutant profiles, source contributions and implications on human health and vegetation. Aziz and Bajwa (2004) attributed the increase in local pulmonary and cardiac illnesses to air pollution and suggested limitations on traffic pollution, efficient traffic management and the development of alternative energy solutions.

2.2 Sampling

Airborne particulate matter (PM10) was collected on Quartz® membrane filters (47 mm, Pall Life Sciences) utilizing an automated high precision air sampler with a PM10 inlet head. The system was run at a nominal volumetric flow rate of 25 L min^{-1}. Flow stability was continually maintained by an in line electronic flow sensor, digital feedback controller and adjustable control valve, to keep volumetric flow within ± 0.1 L min^{-1}. Operational sampling parameters and total flow volumes were monitored and confirmed by a wireless user interface, and an integrated power loss recovery module automatically saved system logs and resumed sampling after an interruption.

Samples were collected from the roof top of one story school building at Kotwali Road near Clock Tower in central Faisalabad (Figure 1). A total of 79 round the clock (24-h) PM10 samples were collected at the frequency of two samples per week for four different seasons, i.e., winter, spring, summer and autumn. Prior to and following sampling, filters were equilibrated in a climate controlled room (20 ± 2 ºC; 40 % relative humidity) for at least 24 h. Gravimetric mass measurements were performed using a microbalance (Sartorius CPA2P-F; readability 0.001 mg). To account for potential background contamination during transport and handling, field and laboratory blank filters were processed following identical conditioning routines, and sample net masses were blank corrected accordingly. After weighing, individual filters were stored in sealed Petri dishes, wrapped with Parafilm®, and refrigerated at 4 ºC prior to chemical analysis.

2.3 Chemical Analysis

https://doi.org/10.5194/egusphere-2026-6556
Preprint. Discussion started: 16 November 2026
© Author(s) 2026. CC BY 4.0 License.

Cation (K^+) and saccharides (Levoglucosan, Mannosan, Galactosan, Arabitol, Mannitol, Erythritol, Inositol, Trehalose, Glucose, Galactose, Fructose, Sucrose, Cellobiose) were extracted from 10 mm filter tickets using 38 mM methanesulfonic acid (MSA; Merck, 99 %) for K^+ and Milli-Q® ultrapure water (18.2 MΩ) for saccharides, followed by 30 minutes of ultrasonic agitation (VWR®), 10 minutes centrifugation at 4000 rpm (Sigma 2-6®) to precipitate insoluble carbon and filter residues, and filtration through 0.45 µm syringe filters (Pall Acrodisc®) prior to injection. Cation quantification (K^+) was performed via isocratic high performance cation exchange chromatography on a Dionex ICS-3000 system equipped with a Spark Marathon® autosampler, guard column, IonPac™ CS16 analytical column (4 × 250 mm), column heater, self-regenerating suppressor (CSRS-500), and conductivity detector using 38 mM MSA as the eluent. Saccharides were determined via high performance anion exchange chromatography with pulsed amperometric detection (HPAEC-PAD; Dionex ICS-3000) using a dual head gradient pump, gradient mixer, CarboPac™ MA1 analytical column (4 × 250 mm), and an electrochemical detector with gold working and reference electrodes under basic gradient elution (1 M NaOH; Carl Roth®). All chromatographic operations, system pressure, and baseline integrity was monitored using Chromeleon™ software.

https://doi.org/10.5194/egusphere-2026-6556
Preprint. Discussion started: 16 November 2026
© Author(s) 2026. CC BY 4.0 License.

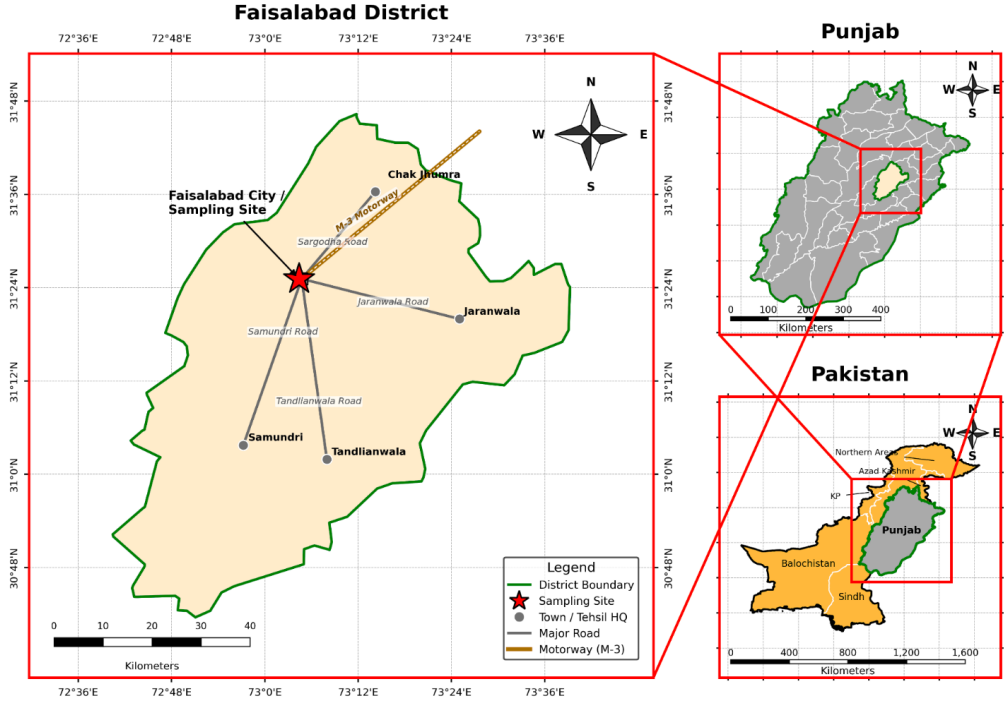


Figure 1 The geographical location of sampling site and Faisalabad district in the political map of Pakistan

https://doi.org/10.5194/egusphere-2026-6556
Preprint. Discussion started: 16 November 2026
© Author(s) 2026. CC BY 4.0 License.

2.4 Meteorology

The regional climate is classified as subtropical with extreme temperature fluctuations and seasonal variations. Summer extends from April through July, with the highest temperatures recorded between May and July, where daily averages range from 27 ºC to 39 ºC and peak temperatures reach up to 48 ºC. Winter starts in November and continues through to February. The coldest temperatures are between December and February, with average daily temperatures between 6 ºC and 21 ºC and minimum temperatures between -1 ºC and 1 ºC. The average annual rainfall in the region is 300 mm of which half is received during the monsoon season of July to August (Pakistan Environmental Protection Agency, 2006).

2.5 HYSPLIT Air Mass & Concentration Weighted Trajectories

To identify the regional air mass transport channels and probable long range source regions that influence the receptor site, 72-h backward trajectories were estimated using the NOAA-HYSPLIT model (Wang et al., 2021; Werden et al., 2023). The trajectories were computed using GDAS meteorological data at an arrival height of 500 meters above ground level utilizing https://www.ready.noaa.gov/HYSPLIT.php. To cluster the trajectories, we used a k-means clustering technique that reduced the total spatial variance which resulted in three different trajectory clusters. Seasonal Concentration Weighted Trajectory (CWT) analysis was performed to systematically investigate the seasonal fluctuations, regional origins and relative strengths of PM10 sources affecting Faisalabad. The CWT model combines backward air mass trajectories with ground level PM10 observations to estimate weighted concentrations for each grid cell (Shao et al., 2026), which represent the influence of meteorology, agricultural cycles, and PBL dynamics on seasonal transport.

2.6 Source Identification of Sugar Compounds

https://doi.org/10.5194/egusphere-2026-6556
Preprint. Discussion started: 16 November 2026
© Author(s) 2026. CC BY 4.0 License.

A Spearman correlation analysis was carried out between PM10, K^+, anhydrous sugars, sugar alcohols, and primary saccharides to assess co-emissions and possible sources (Emygdio et al., 2018; Kolawole et al., 2026; Shao et al., 2026). To investigate the seasonal variability and origins of primary biogenic aerosol particles (PBAPs) and biomass burning tracers in Faisalabad, we applied Principal Component Analysis (PCA) on 13 sugar compounds found in PM10 (Li et al., 2021; Chen and Liu, 2024; Rabhi et al., 2024). Diagnostic concentration ratios of tracer compounds (e.g. Levoglucosan to Mannosan (L/M) and Levoglucosan to water soluble Potassium (L/K^+) were used as robust geochemical fingerprints to differentiate specific biomass burning source types (e.g. hardwood, softwood, crop residues or grasses) (Li et al., 2021; Wang et al., 2021; Ankit et al., 2026). Non-negative matrix factorization (NMF) analysis was applied to identify potential emission sources and to estimate their contributions to atmospheric saccharides. Lee and Seung (1999) proposed NMF, which is similar in spirit to positive matrix factorization (PMF). Both methods decompose an input data matrix (V) into two non-negative matrices, a contribution matrix (W) and a source profile matrix (H) such that $V = WH$, subject to the non-negativity constraints ($W \geq 0$ and $H \geq 0$). However, PMF penalizes negative values to force non-negativity. NMF inherently keeps only non-negative factors. In addition to minimizing the ordinary least squares error, NMF also minimizes the generalized Kullback-Leibler divergence (Shang et al., 2018), leading to more sensitive resolved profiles to the intrinsic features of the input dataset and typically extracting less factors (Zhang et al., 2019). Values below the detection limit (DL) were replaced by half of the DL. NMF was performed on species such as Levoglucosan, Mannosan, Galactosan, Arabitol, Mannitol, Erythritol, Myo-Inositol, Trehalose, Glucose, Galactose, Fructose and Sucrose. Cellobiose was not considered as it was under the detection limit in most of the samples. Measurement uncertainties were estimated to be 0.3 + analytical detection limit ($\sigma = 0.3 + DL$) according to Xie et al. (1999). The constant 0.3 is the logarithm of the geometric standard deviation calculated from the

https://doi.org/10.5194/egusphere-2026-6556
Preprint. Discussion started: 16 November 2026
© Author(s) 2026. CC BY 4.0 License.

normalized concentrations of all measured species, considering measurement variability. A systematic assessment of synoptic transport pathways and regional combustion sources controlling air quality in Faisalabad was performed by combining 72-hour backward air mass trajectories (K-Means cluster analysis, k = 3) with Moderate Resolution Imaging Spectroradiometer (MODIS) active fire counts and trajectory mean Levoglucosan (Levo, ng m^{-3}) concentrations in four seasons. MODIS active fire detections are received via NASA's Fire Information for Resource Management System (FIRMS) at https://earthdata.nasa.gov/firms.

https://doi.org/10.5194/egusphere-2026-6556
Preprint. Discussion started: 16 November 2026
© Author(s) 2026. CC BY 4.0 License.

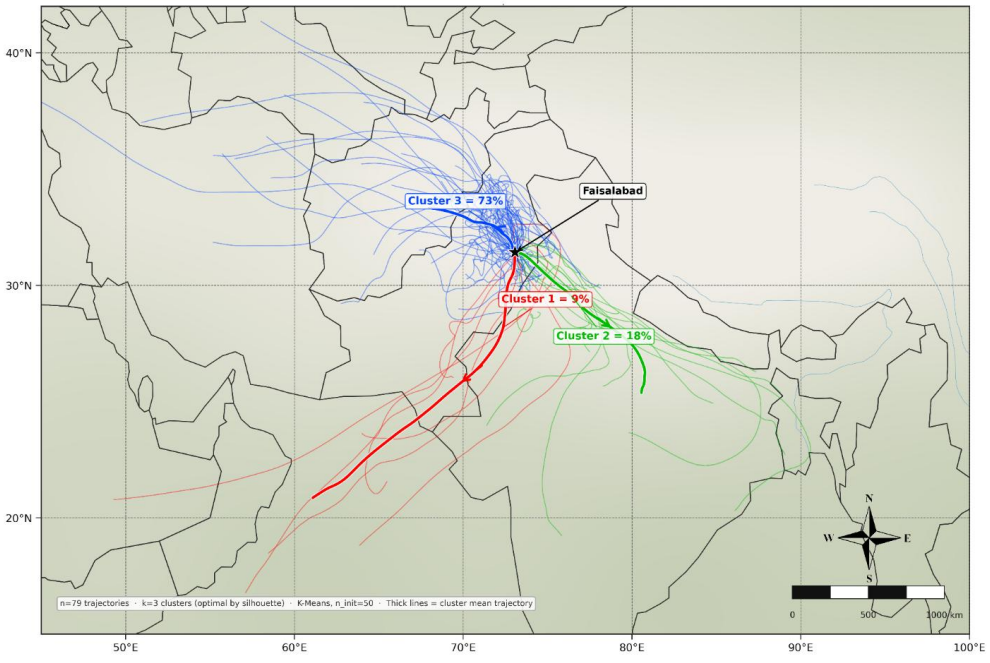


Figure 2 NOAA-HYSPLIT mean clustered 72-h air mass back trajectories arriving at the sampling site (Faisalabad) at 500 m AGL

https://doi.org/10.5194/egusphere-2026-6556
Preprint. Discussion started: 16 November 2026
© Author(s) 2026. CC BY 4.0 License.

2. Results and Discussion

3.1 HYSPLIT Air Mass Back Trajectory Analysis

Figure 2 presents the individual trajectories (thin lines) and the average trajectory for each cluster (bold lines). Cluster 1 (9 %; red trajectory lines) reflects long range, fast moving marine and coastal air masses from Arabian Sea. These air masses moved from the southwest to the receptor location across western India and southeastern Pakistan. The fast speed and vast distance they traveled in that 72-hour period suggests they were carried along by strong synoptic scale air circulation and hence may have transported marine aerosols.

Cluster 2 (18 %; green trajectory lines) includes air masses traveling slower from the southeast and east, originating from the IGP in northern and northwestern India. These routes cross across strongly industrialized, densely populated and intensively farmed areas and hence represent an important route for transboundary contamination. Such air masses are quite likely to bring large amounts of agricultural emissions, biomass burning residues (e.g. crop residue burning), and secondary inorganic aerosols to the receptor site.

Cluster 3 (73 %; blue trajectory lines) is the dominating air mass channel across the study period and is responsible for almost three quarters of all assessed trajectories. These air masses come from the northwest and west and travel over portions of Central Asia, Afghanistan and northern/western Pakistan (particularly Khyber Pakhtunkhwa and Balochistan) before arriving at Faisalabad. The high density of short, closely spaced individual trajectories around the receptor site indicates stagnant, slow moving air conditions in the lower troposphere. This stasis favors the buildup of local urban emissions, vehicle and industrial pollution, and crustal dust from neighboring arid regions. These trajectory characteristics collectively suggest that while local source control is important for air quality management in Faisalabad, regional and transboundary atmospheric movement is an important driver of episodic pollution surges.

https://doi.org/10.5194/egusphere-2026-6556
Preprint. Discussion started: 16 November 2026
© Author(s) 2026. CC BY 4.0 License.

3.2 Concentration Levels of PM10 & K^+

The PM10 concentrations ranged from 169 to 1177 µg m^{-3}, averaging 658 ± 304 µg m^{-3} across the entire sampling campaign. The particulate levels displayed a pronounced seasonal cycle, peaking during Autumn (940 ± 167 µg m^{-3}) and Winter (853 ± 183 µg m^{-3}), while Spring (510 ± 257 µg m^{-3}) and Summer (399 ± 192 µg m^{-3}) were markedly lower as given in Figure 3. All seasonal means were 2.7 to 6.3 folds above the 24-h limit of NEQS (150 µg m^{-3}) by Pak-EPA and NAAQS (150 µg m^{-3}) by USEPA. The total mean was 13 folds above the 24-h guideline (50 µg m^{-3}) by WHO. Reported PM10 concentrations from national, South Asian and international research in the regional and global context are summarized in Table 2. The high concentrations of Autumn and Winter were mostly associated with post harvest agricultural residue burning and home or commercial biomass heating (Chakraborty and Gupta, 2010; Pakbin et al., 2010; Alvi et al., 2018). These emissions were aggravated by poor atmospheric dispersion or stagnant air masses that are characterized by low boundary layer heights and frequent fog spells that also favor secondary aerosol generation (Biswas et al., 2008; Sharma et al., 2014; Shahid et al., 2015). Conversely, the dominant species of Summer PM10 were crustal and road dust resuspension due to high temperatures, dry conditions, winds and dust storms (Stone et al., 2010). The lowest levels of PM10 in general were seen during the precipitation events due to wet deposition and atmospheric scavenging (Budhavant et al., 2009; Shah et al., 2012). Elemental potassium (K^+), a well-known inorganic tracer of biomass burning, paralleled PM10 closely. Concentrations were significantly greater in Winter (14 ± 6 µg m^{-3}) and Autumn (13 ± 5 µg m^{-3}) compared to Spring (7 ± 4 µg m^{-3}) and Summer (4 ± 3 µg m^{-3}) due to increased post harvest residue burning and residential biomass burning during the colder months. Unique seasonal dynamics were seen in general for all chemical species investigated, driven by differences in conventional farming methods, boundary layer mechanics, ambient temperature and biogenic activity.

https://doi.org/10.5194/egusphere-2026-6556
Preprint. Discussion started: 16 November 2026
© Author(s) 2026. CC BY 4.0 License.

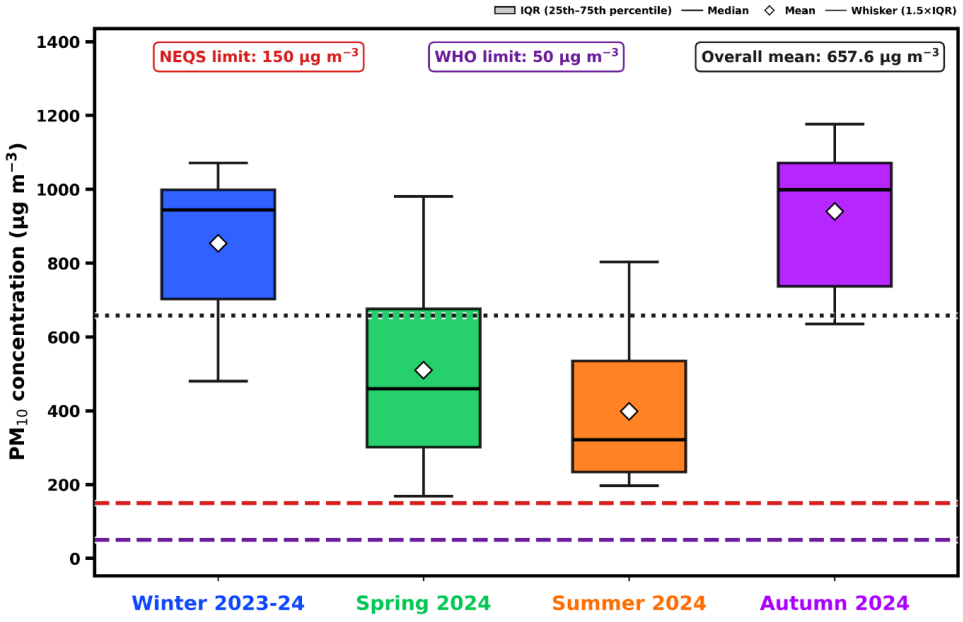


Figure 3 Observed PM10 concentration levels during the sampling campaign in comparison with NEQS and WHO air quality guidelines

https://doi.org/10.5194/egusphere-2026-6556
Preprint. Discussion started: 16 November 2026
© Author(s) 2026. CC BY 4.0 License.

309 **Table 2** Comparison of the concentrations of PM10 of current study to the nation-wide, regional, and international studies

Sampling Site/Location	Country	Sampling Duration	Sampling Year	Concentration of PM10 (ugm^{-3})	Reference
Nazria Pakistan Square, Faisalabad	Pakistan	24 h	2016-2017	800	Aslam et al., 2020
Lahore Urban Area	Pakistan	-	2007	996	Ghauri et al., 2007
Industrial Area, Lahore	Pakistan	10 h	2020	300	Rehman et al., 2023
Canal Bank Road, Lahore	Pakistan	24 h	2018-2019	284	Khan et al., 2024
Lahore City Center	Pakistan	Dec-Feb	2019	105	Ahmad et al., 2025
Southern Lahore	Pakistan	24 h	2021	80	Shahzadi et al., 2024
Gujranwala	Pakistan	-	-	201	Ashraf et al., 2022
Rawalpindi	Pakistan	8 h	2019	311	Tabinda et al., 2019
Islamabad	Pakistan	24 h	2016	121-184	Bulbul et al., 2018
Nowshera	Pakistan	24 h	2018	505	Zeb et al., 2022
Peshawar	Pakistan	24 h	2016	638	Zeb et al., 2018
Charsadda	Pakistan	-	2019	254	Ahmad et al., 2019
Quetta	Pakistan	-	2015	700	Ishtiaq et al., 2015
Karachi	Pakistan	24 h	2017	302	Ghauri et al., 2007
Manali	India	Nov 2014-May 2016	2014-2016	103-131	Panda and Nagendra, 2018
Gurugram	India	-	2017	440	Rahman et al., 2020
Delhi	India	24 h	2020	826	Singh et al., 2025
Ghaziabad	India	Seasonal	2018-19	384	Gupta et al., 2021
Kanpur	India	Seasonal	2015-16	96-401	Rajput et al., 2019
Ahmedabad	India	Dec 2006-Jan 2007	2006-2007	171	Rengarajan et al., 2011
Varanasi	India	24 h	2014-2017	268	Murari et al., 2020
Patna	India	Jan-Dec 2018	2018	90-238	Devi et al., 2024
Bharatpur	India	24 h	2022-23	638	Pradhan et al., 2025
Murshidabad	India	24 h	2018-2019	539	Arif and Parveen, 2021
Pune	India	Yearly	2012	121	Yadav et al., 2015
Kolkata	India	24 h	-	445	Kumar et al., 2024

Brahmaputra Valley	India	Dec 2010-Oct 2014	2010-2014	22-96	Bhuyan et al., 2018
Bengaluru	India	24 h	-	96	Sowmya et al., 2024
Lalitpur	Nepal	23 h	2018	174-377	Islam et al., 2022
Rajshahi West	Bangladesh	-	-	250-300	Majumder et al., 2025
Khulna	Bangladesh	24 h	2018-2020	415	Saju et al., 2023
Savar	Bangladesh	24 h	-	699	Begum et al., 2009
Dhaka	Bangladesh	24 h	2024	73-416	Pabel et al., 2025
Postogola	Bangladesh	24 h	Nov 2018-Aug 2019	341	Gulshan et al., 2021
Tehran	Iran	Yearly	2016	180	Yunesian et al., 2019
Qom	Iran	-	-	90	Nadali et al., 2020
Ahvaz	Iran	24 h	2009	320	Hamidi et al., 2025
Ilam city	Iran	24 h	2012-2013	344	Amarloei et al., 2020
Across UAE Cities	United Arab Emirates	Annual	2008-2016	122-153	World Health Organization, 2018
Doha	Qatar	-	-	145	Javed et al., 2019
Kuwait City Centre	Kuwait	24 h	Oct 2017-Nov 2019	137	Hopke et al., 2026
Qassim region	Saudi Arabia	Jul 2020-June 2021	2020-2021	152	Alnagran et al., 2023
Jeddah	Saudi Arabia	-	-	87	Khodeir et al., 2012
Beirut	Lebanon	-	-	51	Farah et al., 2018
Across Egyptian Cities	Egypt	Annual	2008-2016	249-284	World Health Organization, 2018
Zhengzhou	China	Monthly	2020	97	Liang et al., 2022
North China Plain	China	Annual	2015	120	Zhai et al., 2023
Beijing	China	12 h	2014	200	Lin et al., 2016
Huangshi City	China	Apr 2018	2018	115	Zhang et al., 2022
Guangzhou	China	Aug-Sep 2004	2004	138	Wang et al., 2006b
Shanghai	China	Yearly	2013-14	109	Zhang et al., 2015
Shenyang, Northern China	China	1998-2009	1998-2009	154	Dong et al., 2012
Mae Sai	Thailand	24 h	2020	396	Supasri et al., 2023
Hanoi	Vietnam	Annual	2001-2004	162	Kim Oanh et al., 2006

https://doi.org/10.5194/egusphere-2026-6556
Preprint. Discussion started: 16 November 2026
© Author(s) 2026. CC BY 4.0 License.

Taiwan	Taiwan	18 years	1995-2013	62	Chen et al., 2017
Seoul	South Korea	24 h	2015	89	Allabakash et al., 2022
Yeongam	South Korea	24 h	2015-2017	80-150	Son et al., 2020
Kota Samarahan	Malaysia	24 h	2019-2020	196	Othman et al., 2022
Manila	Philippines	Annual	2001-2004	55	Kim Oanh et al., 2006
Jakarta	Indonesia	-	2000-2016	38-112	Kusumaningtyas et al., 2018
Bandung	Indonesia	-	2001-2004	106	Kim Oanh et al., 2006
West Surabaya	Indonesia	24 h	2019-2020	27	Wen et al., 2023
Switzerland	Switzerland	9 years	2003-2012	23	Fleury et al., 2021

https://doi.org/10.5194/egusphere-2026-6556
Preprint. Discussion started: 16 November 2026
© Author(s) 2026. CC BY 4.0 License.

https://doi.org/10.5194/egusphere-2026-6556
Preprint. Discussion started: 16 November 2026
© Author(s) 2026. CC BY 4.0 License.

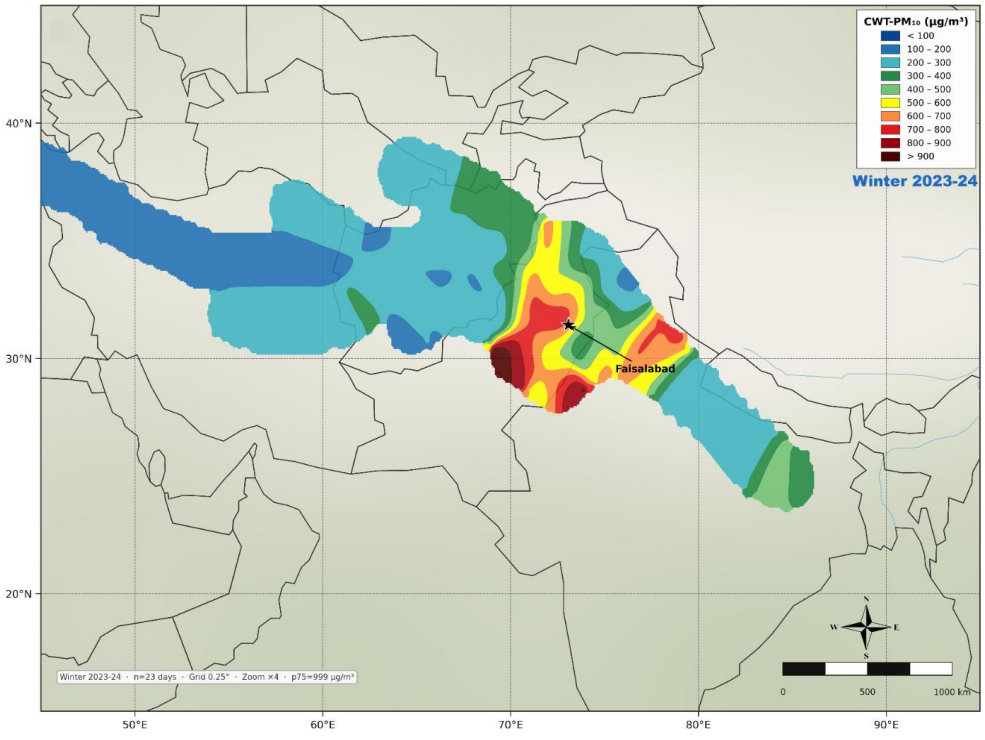


Figure 4 Spatial distribution of concentration weighted trajectories (CWT) for PM10 during Winter

https://doi.org/10.5194/egusphere-2026-6556
Preprint. Discussion started: 16 November 2026
© Author(s) 2026. CC BY 4.0 License.

3.3 Concentration Weighted Trajectory (CWT) Analysis

During Winter, a shallow continental PBL and frequent thermal inversions severely limited atmospheric dispersion, trapping emissions locally to yield extreme CWT values of 700–800 µg m^{-3} (red) directly over Faisalabad and exceeding 900 µg m^{-3} (deep maroon) to its southwest as shown in Figure 4. Upwind transboundary air masses arriving at the receptor from northwestern India (traveling along the Indo-Gangetic Plain) carried heavy industrial, brick kiln, and secondary aerosol emissions to Faisalabad, resulting in high CWT values of 600–800 µg m^{-3} (orange/red). Concurrently, backward trajectories tracking northwest show that clean air masses originating in Central Asia (~200 µg m^{-3}) contained substantial crustal dust while passing over the hyper arid terrains of Balochistan and southern Afghanistan, arriving at the receptor with moderate CWT values of 300–500 µg m^{-3} (green/yellow).

As spring transitioned with rising temperatures and an expanding PBL, the extreme source hotspots contracted closer to the east and northeast of Faisalabad (Figure 5). Long range back trajectories arriving from the west and northwest (across Iran and Afghanistan) became exceptionally clean with CWT values < 200 µg m^{-3} (blue), indicating a minimal role for long range western dust. Instead, moderate spring contributions from 300–500 µg m^{-3} (green) were dominated by air masses passing over localized wheat harvesting and land preparation activities in central Punjab.

Summer exhibited the lowest overall CWT values, as a deep and well mixed PBL along with monsoonal wet scavenging kept regional upwind corridors below 200 µg m^{-3} (deep blue) (Figure 6), confining moderate contributions ranged from 300 to 500 µg m^{-3} (green/yellow) to short range air masses, traversing the immediate vicinity of Faisalabad, where convective dust storms resuspended dry local soil.

In autumn, regional pollution experienced a dramatic resurgence; falling temperatures and intensive crop residue burning across Pakistani and Indian Punjab heavily loaded incoming air masses from the east and southeast, driving CWT values to 700–900 µg m^{-3}

https://doi.org/10.5194/egusphere-2026-6556
Preprint. Discussion started: 16 November 2026
© Author(s) 2026. CC BY 4.0 License.

(orange/red/maroon) (Figure 7). Additionally, slow moving air masses tracking northward along the lower Indus basin collected regional dust and industrial emissions with CWT values 300–500 µg m^{-3} (green), while clean northwestern back trajectories (200–300 µg m^{-3}) confirmed that the autumn crisis was overwhelmingly driven by regional biomass combustion rather than long range transport of crustal dust.

https://doi.org/10.5194/egusphere-2026-6556
Preprint. Discussion started: 16 November 2026
© Author(s) 2026. CC BY 4.0 License.

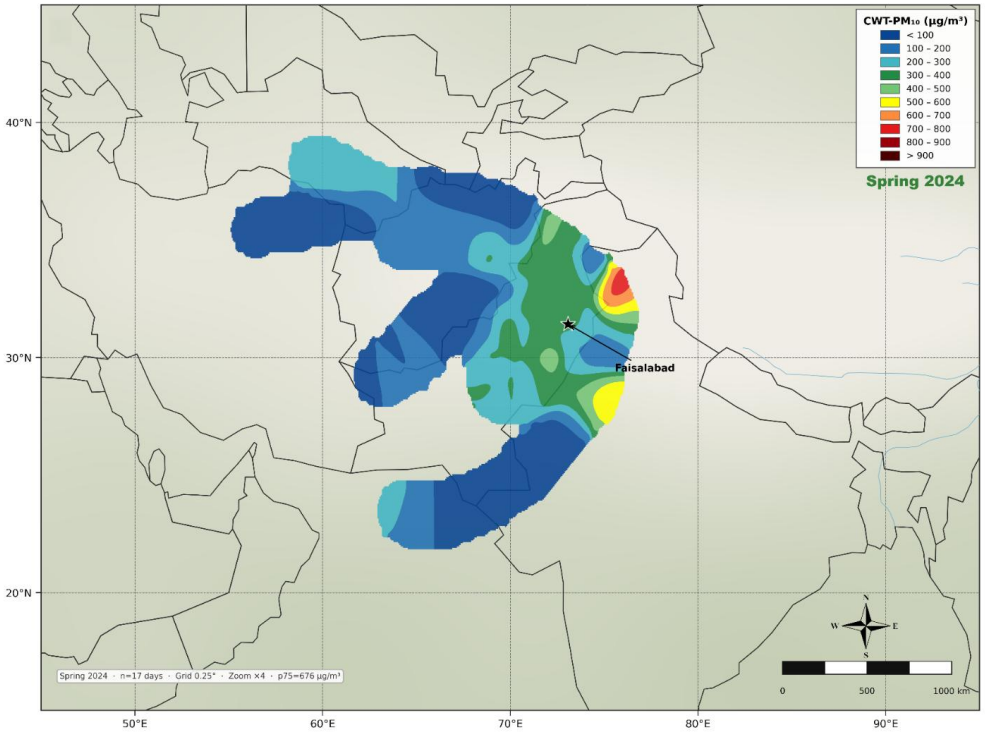


Figure 5 Spatial distribution of concentration weighted trajectories (CWT) for PM10 during Spring

https://doi.org/10.5194/egusphere-2026-6556
Preprint. Discussion started: 16 November 2026
© Author(s) 2026. CC BY 4.0 License.

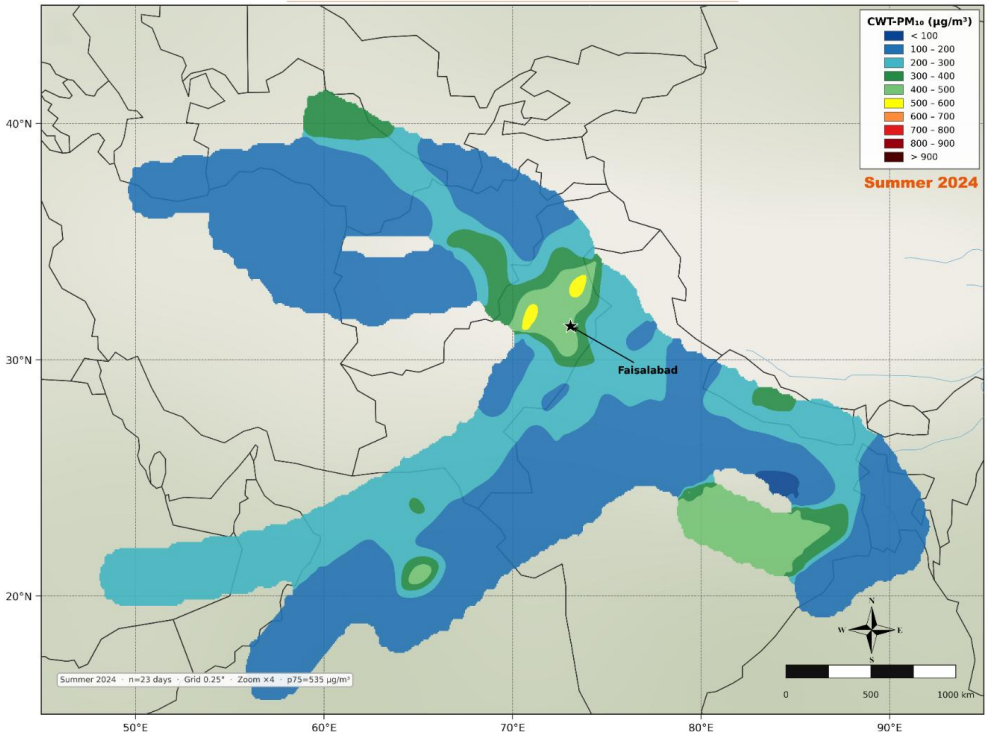


Figure 6 Spatial distribution of concentration weighted trajectories (CWT) for PM10 during Summer

https://doi.org/10.5194/egusphere-2026-6556
Preprint. Discussion started: 16 November 2026
© Author(s) 2026. CC BY 4.0 License.

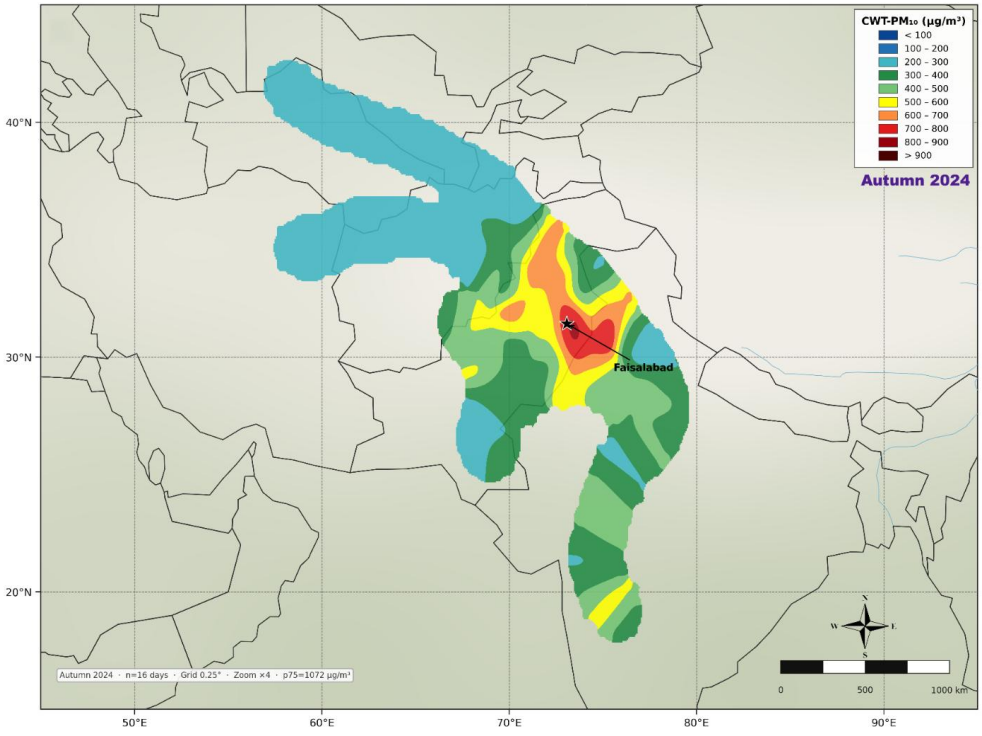


Figure 7 Spatial distribution of concentration weighted trajectories (CWT) for PM10 during Autumn

https://doi.org/10.5194/egusphere-2026-6556
Preprint. Discussion started: 16 November 2026
© Author(s) 2026. CC BY 4.0 License.

3.4 Concentration Levels of Sugars

Among the analyzed organic compound classes, Anhydrosugars were the most dominant category, representing 72 % of total quantified sugar species. Levoglucosan, the most specific biomass burning marker, was highest in Autumn (3283 ± 1334 ng m^{-3}) and Winter (2530 ± 964 ng m^{-3}), roughly 3.5 to 8.5 times its Summer (386 ± 207 ng m^{-3}) and Spring (874 ± 526 ng m^{-3}) levels respectively, as illustrated in Figure 8. Mannosan followed the same order (Autumn 101 ± 47 ng m^{-3}; Winter 99 ± 36 ng m^{-3}; Spring 29 ± 20 ng m^{-3}; Summer 26 ± 23 ng m^{-3}). Galactosan was strongly seasonal to the point of near absence in warm months: 71 ± 32 ng m^{-3} in Winter and 87 ± 45 ng m^{-3} in Autumn, but only 11 ± 19 ng m^{-3} in Spring and entirely below detection in all Summer samples, consistent with the near total suppression of open burning during the hot, and wet season. The overwhelming prevalence of Levoglucosan suggests the thermal breakdown of cellulose during biomass burning as the single most important source of aerosol bound organic carbon in this agro-industrial region.

Primary saccharides were the second most abundant class, making up 17 % of total sugars. Glucose, the predominant primary sugar, was highest in Winter (250 ± 92 ng m^{-3}) and lowest in Spring (96 ± 83 ng m^{-3}), with Summer (147 ± 143 ng m^{-3}) and Autumn (168 ± 188 ng m^{-3}) intermediate but highly right skewed. Galactose ranged from 15 ± 12 ng m^{-3} in Winter and down to 3 ± 6 ng m^{-3} in Summer. Fructose peaked in Winter (87 ± 41 ng m^{-3}) and was lowest in Summer (34 ± 32 ng m^{-3}). Sucrose showed no strong seasonal ordering (Summer 78 ± 90 ng m^{-3} highest; Autumn 46 ± 57 ng m^{-3} lowest), consistent with a mixed plant debris or pollen source active across seasons. Trehalose, associated with soil or fungal resuspended biological material, was highest in Autumn (126 ± 46 ng m^{-3}) and lowest in Summer (76 ± 30 ng m^{-3}). Cellobiose was the most sporadically detected species overall with means ranging from 9 ± 20 ng m^{-3} (Summer) to 43 ± 69 ng m^{-3} (Autumn).

https://doi.org/10.5194/egusphere-2026-6556
Preprint. Discussion started: 16 November 2026
© Author(s) 2026. CC BY 4.0 License.

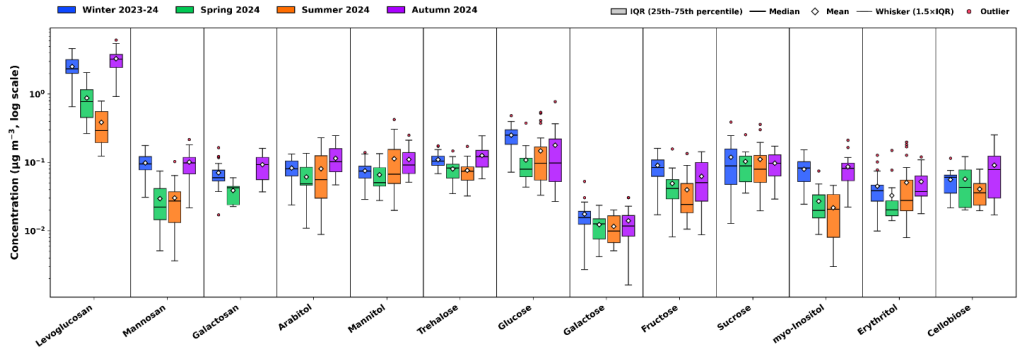


Figure 8 Mass concentrations of anhydrosugars, primary sugars, and sugar alcohols recorded in PM10 samples during the study period

https://doi.org/10.5194/egusphere-2026-6556
Preprint. Discussion started: 16 November 2026
© Author(s) 2026. CC BY 4.0 License.

Sugar Alcohols constituted the 3rd fraction with 11 % of total sugar mass. Fungal spore tracers such as Arabitol and Mannitol showed unique seasonal trend, peaking in Autumn (Arabitol 114 ± 54 ng m^{-3}; Mannitol 110 ± 56 ng m^{-3}), while Spring was lowest for both (Arabitol 61 ± 31 ng m^{-3}; Mannitol 66 ± 3 ng m^{-3}). Myo-Inositol mirrored the anhydrosugar pattern with Autumn (86 ± 46 ng m^{-3}) and Winter (76 ± 38 ng m^{-3}) highest, and Summer lowest (21 ± 14 ng m^{-3}). Erythritol, in contrast stayed relatively flat across seasons (48-52 ng m^{-3}). The relatively narrow Winter to Autumn spread for these species (compared to the 3 to 8 times seasonal swing in the Anhydrosugars) supports the conclusion that Summer is the most biologically (fungal spore or bioaerosol) driven season. Concentrations of various sugar compounds of this study are given in Table 3, while reports from the regional and global context are summarized in Table 4 for comparison.

3.5 Seasonal Relative Contribution of Sugars

The proportional distribution of sugar compounds in PM10 changes noticeably with the seasons due to shifts in emissions, farming practices, and weather (Figure 9). Anhydrosugars overwhelmingly dominate during the cooler months, making up 81.1 % of total sugars in Autumn and 76.2 % in Winter, which directly tracks with the highest PM10 levels. Autumn's high levels are driven by widespread rice straw burning across the Indo-Gangetic Plain, which releases Levoglucosan, Mannosan, and Galactosan from burning cellulose (Rajput et al., 2014; Nirmalkar et al., 2015a; Fu et al., 2024). In Winter, this high share persists due to residential wood heating, biomass fired brick kilns, and cold air inversions that trap pollution near the ground (Gonçalves et al., 2021; Islam et al., 2021; Shao et al., 2026). Anhydrosugars decrease to 65.8 % in Spring and a minimum of 40.3 % in Summer due to declining open burning and increasing temperatures allowing biological sources to grow. Primary saccharides are highest in Summer at 34.0 %, driven by vigorous plant growth, pollen release and soil dust thrown up by wheat harvesting and tilling.

Table 3 Statistical data about PM10, K^+ and sugar compounds during Winter, Spring, Summer, and Autumn

Specie	Overall		Winter 2023-24		Spring 2024		Summer 2024		Autumn 2024	
	Avg ± SD	Range	Avg ± SD	Range	Avg ± SD	Range	Avg ± SD	Range	Avg ± SD	Range
PM10*	658 ± 304	169 - 1177	853 ± 183	480 - 1072	510 ± 257	169 - 981	399 ± 192	197 - 803	940 ± 167	635 - 1177
K^+*	9 ± 6	1 - 25	14 ± 6	1 - 22	7 ± 4	2 - 14	4 ± 3	1 - 10	13 ± 5	7 - 25
Sugars**										
Levo	1668 ± 1438	124 - 6172	2530 ± 964	653 - 4638	874 ± 526	263 - 2064	386 ± 207	124 - 790	3283 ± 1334	920 - 6172
Arab	83 ± 51	BDL - 247	82 ± 26	24 - 133	61 ± 31	11 - 136	78 ± 64	BDL - 229	114 ± 54	47 - 247
Mans	62 ± 49	BDL - 217	99 ± 36	31 - 177	29 ± 20	5 - 75	26 ± 23	BDL - 103	101 ± 47	22 - 217
Treh	97 ± 39	32 - 245	110 ± 29	68 - 175	80 ± 30	35 - 147	76 ± 30	32 - 172	126 ± 46	58 - 245
Mant	93 ± 67	20 - 425	75 ± 27	29 - 140	66 ± 31	28 - 134	113 ± 97	20 - 425	110 ± 56	52 - 251
Galn	40 ± 46	BDL - 165	71 ± 32	17 - 165	11 ± 19	BDL - 60	BDL	BDL	87 ± 44	BDL - 161
Gluc	170 ± 143	BDL - 777	250 ± 92	72 - 484	96 ± 83	BDL - 377	147 ± 143	33 - 540	168 ± 188	BDL - 777
Gals	9 ± 10	BDL - 53	15 ± 12	BDL - 53	9 ± 7	BDL - 24	3 ± 6	BDL - 20	14 ± 8	2 - 31
Fruc	53 ± 45	BDL - 161	87 ± 41	BDL - 161	43 ± 37	BDL - 157	34 ± 32	BDL - 135	48 ± 48	BDL - 143
Sucr	65 ± 84	BDL - 389	75 ± 98	BDL - 389	49 ± 69	BDL - 255	78 ± 90	BDL - 360	46 ± 57	BDL - 173
Inos	50 ± 43	BDL - 211	76 ± 38	BDL - 153	25 ± 18	BDL - 75	21 ± 14	BDL - 46	86 ± 46	22 - 211
Eryt	46 ± 40	8 - 199	45 ± 27	10 - 128	33 ± 33	14 - 150	51 ± 53	8 - 199	52 ± 32	18 - 120
Cell	22 ± 42	BDL - 252	28 ± 33	BDL - 115	13 ± 31	BDL - 122	9 ± 20	BDL - 80	43 ± 69	BDL - 252

Levo = Levoglucosan, Arab = Arabitol, Mans = Mannosan, Treh = Trehalose, Mant = Mannitol, Galn = Galactosan, Gluc = Glucose, Gals = Galactose, Fruc = Fructose, Sucr = Sucrose, Inos = Inositol, Eryt = Erythritol, Cell = Cellobiose, BDL = Below Detection Limit

*Values in μg m^{-3}

**Values in ng m^{-3}

https://doi.org/10.5194/egusphere-2026-6556
Preprint. Discussion started: 16 November 2026
© Author(s) 2026. CC BY 4.0 License.

EGUsphere Preprint repository

416 **Table 4** Comparison of the concentrations of sugar compounds of current study to the regional, and international studies

Study Area	Study Period	PM10	Levo	Arab	Mans	Treh	Mant	Gals	Gluc	Galn	Fruc	Sucr	Inos	Eryt	Reference
Lahore, Pakistan	13 Mar to 16 Apr, 2006	459	9 %	—	—	—	—	—	—	—	—	—	—	—	Zhang et al., 2008b
Dal Lake, Srinagar,	Mar, 2023	—	716 ± 64	—	292 ± 51	—	—	—	—	280 ± 46	—	—	—	—	Ankit et al., 2026
New Delhi, India	Nov, 2006 to Feb, 2007	440 ± 95*	1977 ± 971	51 ± 22	179 ± 156	76 ± 45	45 ± 24	—	173 ± 112	262 ± 207	44 ± 31	485 ± 520	20 ± 11	—	Li et al., 2014
Lumbini, Nepal	20 Dec, 2017 to 1 Jan, 2018	157.8 ± 66.0	3747 ± 1106	—	—	—	—	—	—	—	—	—	—	11.0 ± 2.9	Islam et al., 2022
Kathmandu, Nepal	18-27 Jan, 2018	194–309	1700–2536	—	—	—	—	—	—	—	—	—	—	—	Islam et al., 2022
Central Himalayas	Aug, 2009 to Jul, 2010	—	19 ± 38	1.9 ± 1.7	1.3 ± 2.3	1.8 ± 1.3	1.6 ± 1.3	—	6.6 ± 5.7	0.85 ± 1.5	3.5 ± 3.3	2.3 ± 4.0	0.30 ± 0.26	0.64 ± 0.60	Fu et al., 2026
Raipur, Central India	2014	240 ± 63	2210 ± 2381	29.8 ± 18.9	148.1 ± 130.9	36.9 ± 23.8	26.5 ± 33.6	—	47.4 ± 22.6	59.4 ± 50.7	10.8 ± 11.2	38.6 ± 46.1	9.3 ± 14.4	—	Ramteke et al., 2022
Chhattisgarh, India	Jan to Dec, 2006	246 ± 68	0.31 to 31000	—	0.01 to 4180	9.0	—	—	37.0	1.6 to 3600	—	198.0	21.0	—	Giri et al., 2013
Chhattisgarh, India	Dec, 2019	—	140 ± 107	4 ± 2	18 ± 17	2 ± 2	7 ± 5	—	16 ± 22	24 ± 25	6 ± 4	13 ± 17	30 ± 33	—	Ramteke et al., 2022
Mahanadi Riverside Basin	Oct to Nov, 2011	388.9	3250	440	—	1840	3300	800	5840	—	—	—	320	240	Nirmalkar et al., 2015b
Chennai, India	23 Jan to 6 Feb, 2007	—	112	1.05	13.4	1.22	0.54	—	3.86	8.07	1.51	2.06	0.48	2.74	Fu et al., 2010
Lincang, China	8 Mar to 9 Apr, 2019	41.8 (TSP)	287.7	5.8	31.6	13.8	14.7	—	31.2	2.5–5.5	24.6	86.4	5.8	11.1	Wang et al., 2021
Baoji, China	8-10 Apr, 2008	410	261	16	15	20	13	—	112	30	120	473	7.6	—	Xie et al., 2010
Chongqing, China	Jun to Jul, 2003	404 (TSP)	2519	0.2	—	20	1.4, 1.8	—	52.0, 51.0	—	6.3	200	0.1	—	Wang et al., 2006a
Inland China	19 May to 10 Jun, 2004	—	44	—	—	1	2	—	5	—	1	—	—	—	Wang et al., 2007
Xi'an, China	Jan to Feb, 2009	531 ± 156*	576 ± 99	38 ± 18	130 ± 69	9.3 ± 4.3	17 ± 7.9	—	74 ± 35	172 ± 77	44 ± 18	60 ± 63	6.3 ± 3.5	—	Li et al., 2014
Xi'an, China	13 to 14 Jan, 2003	—	2915	0.7	—	42	3.2	—	75	—	12	191	0.1	—	Wang et al., 2006a
Central China (Summit of Mt. Hua)	11-22 Jan, 2009	54 ± 24	65 ± 30	3.0 ± 2.0	7.8 ± 5.4	2.5 ± 2.2	2.2 ± 1.8	—	5.5 ± 4.6	12 ± 6.8	5.4 ± 5.0	2.8 ± 2.6	0.3 ± 0.3	—	Li et al., 2012
Beijing, China	3-31 Aug, 2007	—	34–149	2.8–5.6	7.8	0.1–1.6	2.2–6.3	—	—	5.3	—	—	—	—	Yang et al., 2016
Beijing	Jul, 2002 to Jul, 2003	169 ± 108	307 ± 345	1	—	—	1.1	—	—	—	—	—	—	—	Zhang et al., 2008a
Urban Beijing	Nov, 2012 to Jan, 2013	—	54.43	—	6.14	—	—	—	—	5.47	—	—	—	—	Liang et al., 2016
Guangzhou, China	Jun-Jul, 2003	247 (TSP)	872	0.1	—	3.5	0.8	—	15	—	2.4	75	—	—	Ma et al., 2009
Hong Kong, China	Jun-Jul, 2003	71(TSP)	133.2	0.1	—	1.3	0.4	—	1.2	—	0.2	11.6	—	—	Wang et al., 2006a
Selangor, Malaysia	7 to 13 Jan, 2009	48.3 ± 14.3*	389.98 ± 57.98	—	—	—	—	—	—	—	—	—	—	—	Latif et al., 2011
Nanjing, China	12-24 Oct, 2007	226 ± 66*	689 ± 243	21 ± 3.6	—	17 ± 1.9	24 ± 4.2	—	44 ± 8.3	—	32 ± 13	31 ± 19	7.0 ± 2.8	—	Wang et al., 2011
East coast China	25 Dec, 2002 to 06 Jan, 2003	—	41	—	—	0	0	—	36	—	18	17	2	—	Wang et al., 2007
Changzhou, China	1-18 Jan, 2017	—	184.5 ± 128.9	4.4 ± 2.8	17.1 ± 11.0	—	42.6 ± 39.0	—	6.7 ± 3.7	8.4 ± 4.0	—	—	—	3.0 ± 1.7	Shao et al., 2026

https://doi.org/10.5194/egusphere-2026-6556
Preprint. Discussion started: 16 November 2026
© Author(s) 2026. CC BY 4.0 License.

Shanghai, China	23 Oct, 2011 to 20 Aug, 2012	—	111	8.5	17.4	—	14.8	—	—	—	21.4	93.8	3.7	3.0	Li et al., 2016a
Shanghai, China	Dec, 2013 to Jan, 2015	—	232	—	—	—	5–160	—	—	—	—	38–380	—	—	Li et al., 2016b
East China Sea (Huaniao Island)	23 Oct, 2011 to 20 Aug, 2012	—	31.5	1.9	7.8	—	2.5	—	—	—	2.1	3.2	0.1	0.8	Li et al., 2016a
Yunlin County, Taiwan	21 Jun to 08 Jul, 2007	124	1116	—	8.3	—	—	—	—	9.9	—	—	—	—	Engling et al., 2013
Taiwan	2010	46.3 ± 2.68*	21.7	—	1.5	—	—	—	—	3.1	—	—	0.76	—	Tsai et al., 2010
Krakow, Poland	21 Apr, 2018 to 19 Mar, 2019	38.3–107.4	1950	—	—	—	—	—	—	—	—	—	—	—	Skiba et al., 2024
Seoul, South Korea	April 2010 to April 2011	—	387.49	—	—	—	—	5.06	64.32	—	18.17	186.13	—	—	Choi et al., 2016
Jeju Island, Korea	Apr, 2001 to Mar, 2002	—	38	6.7	—	15	5.5	—	18	—	11	245	—	—	Fu et al., 2012
Daejeon, Korea	8 Oct to 3 Dec, 2012	—	180 ± 110	—	27 ± 16	—	—	—	—	—	—	—	—	—	Jung et al., 2014
Vienna, Austria	2004	—	15–200	15-45	—	—	20–80	—	—	—	—	—	—	—	Caseiro et al., 2007
Cosenza, Italy	—	83.10*	9430	—	1850	—	—	—	—	—	—	—	1440	—	Paris et al., 2024
Prague, Republic	Spring, 2004 to Spring, 2005	—	495.8 ± 5.4	—	100.5 ± 1.6	—	—	—	—	35.3 ± 0.8	—	—	—	—	Louchouarn et al., 2009
Rome, Italy	—	170.2 (TSP)	40260	1680	2240	—	2740	—	—	—	—	—	1270	2130	Paris et al., 2024
San Pietro, Northern Italy	2012-2013	34.6 (TSP)	252.9 ± 110.7	—	61.5 ± 27.2	5.3 ± 5.6	6.3 ± 4.9	3.1 ± 1.3	5.4 ± 1.4	32.0 ± 15.4	—	2.6 ± 1.2	—	2.1 ± 1.9	Pietrogrande et al., 2014
Germany	Feb, 2008	—	299	3.8	52	—	57	0.6	8.7	28	—	—	—	1.4	Iinuma et al., 2009
Norway	30 Jan to 15 Mar, 2002	—	605	5.3	167	13	4.2	—	22	4.0	11	95	3.4	—	Yttri et al., 2007
Sapporo, Northern Japan	1 May to 23 Jul , 2005	12–48*	16	19	—	12	16	—	28	—	14	90	9.8	—	Aggarwal and Kawamura
Hokkaido, Japan	13-15 Aug, 2001	—	7.3	16	1.0	3.7	13	—	16	0.3	3.0	4.3	0.4	54	Fu and Kawamura, 2011
Bouismail, Algeria	Jul to Nov, 2012	—	117.3 ± 8.3	31.7 ± 5.2	17.2 ± 1.2	—	21.0 ± 2.7	4.6 ± 0.9	8.2 ± 1.6	3.5 ± 0.4	—	—	—	—	Rabhi et al., 2025
Coimbra, Portugal	Dec, 2018 to Mar, 2019	32.3	692	36.4	115	—	42.3	—	—	45.4	—	—	—	—	Gonçalves et al., 2021
Ogijo, Nigeria	Oct 21-27, 2021	109 ± 38	126 ± 99	—	212 ± 29	—	—	—	—	—	—	—	—	—	Kolawole et al., 2026
Maine, USA	25 Jun to 9 Jul, 2002	—	55.1	5.4	10.4	6.8	6.7	22.2	50.1	2.6	1.4	1.5	—	—	Medeiros et al., 2006
Sao Paulo, Brazil	16 May, 2015 to 9 Jul, 2015	28.2	231.9	11.7	21.8	—	23.3	—		5.5	—	—	—	—	Emygdio et al., 2018

Levo = Levoglucosan, Arab = Arabitol, Mans = Mannosan, Treh = Trehalose, Mant = Mannitol, Gals = Galactose, Gluc = Glucose, Galn = Galactosan, Fruc = Fructose, Sucr = Sucrose, Inos = Inositol, Eryt = Erythritol

* = PM2.5

PM10, PM2.5, TSP = Values in ug m^{-3}

All Sugar Compounds = Values in ng m^{-3}

https://doi.org/10.5194/egusphere-2026-6556
Preprint. Discussion started: 16 November 2026
© Author(s) 2026. CC BY 4.0 License.

https://doi.org/10.5194/egusphere-2026-6556
Preprint. Discussion started: 16 November 2026
© Author(s) 2026. CC BY 4.0 License.

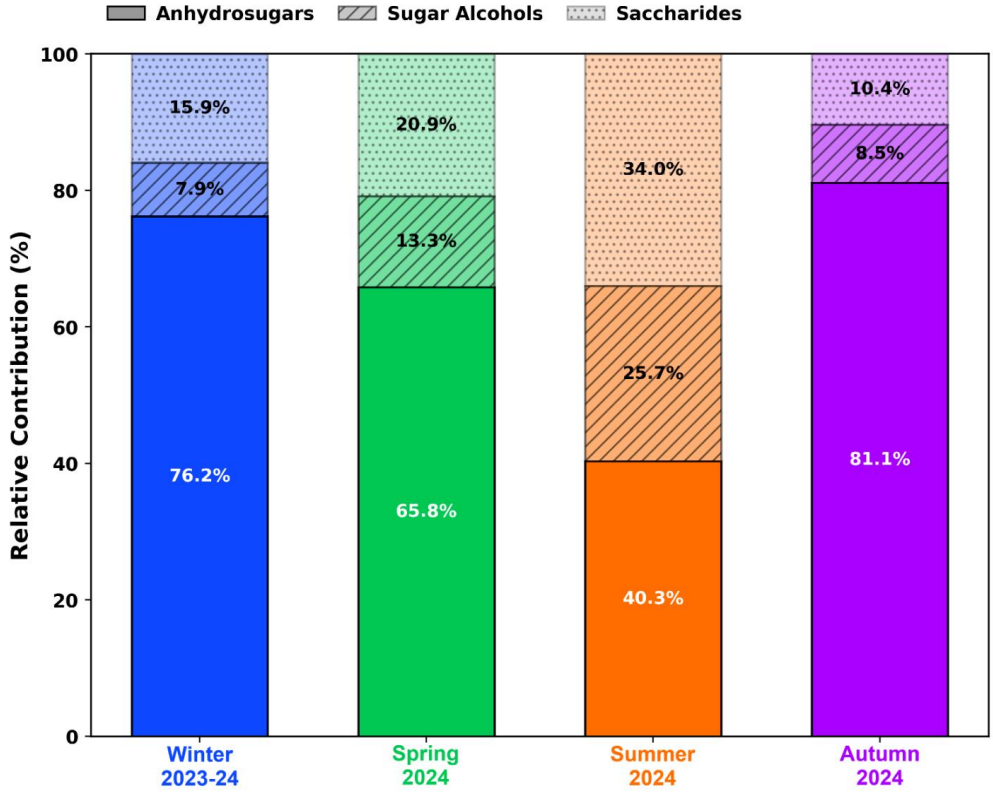


Figure 9 Seasonal relative contribution (%) of anhydrosugars, sugar alcohols, and primary saccharides to total quantified sugars in ambient PM10

https://doi.org/10.5194/egusphere-2026-6556
Preprint. Discussion started: 16 November 2026
© Author(s) 2026. CC BY 4.0 License.

In Summer, Sugar Alcohols too have their largest share at 25.7 %, as warmer and humid weather promotes fungal sporulation and microbial activity.

3.6 Inter-Species Correlations

The most significant feature of correlation matrix is a very large positive cluster encompassing PM10, K^+ and anhydrosugars as shown in Figure 10. Levoglucosan was most highly associated to both PM10 (r = 0.77) and K^+ (r = 0.76). Levoglucosan is formed only during the thermal degradation of cellulose and is closely connected with biomass burning, indicating that it is a major contributor to particle increases (Cheng et al., 2013; Gonçalves et al., 2021; Rabhi et al., 2024; Ankit et al., 2026). The three biomass burning tracers are highly correlated with each other (Levoclucosan vs. Mannosan, r = 0.88, Levoglucosan vs. Galactosan, r = 0.94, and Mannosan vs. Galactosan, r = 0.84), indicating a highly consistent co-emitted tracer profile emitted into the air from regional agricultural crop residue burning and residential wood combustion (Li et al., 2016a, b; Wang et al., 2021). Further, Myo-Inositol showed significant positive correlation with Levoglucosan, Mannosan, Galactosan and K^+ (r = 0.88, 0.83, 0.83 and 0.72, respectively) which implies that its atmospheric pathway is closely associated with thermal volatilization during open field burning (Fu et al., 2010; Li et al., 2012; Nirmalkar et al., 2015b; Wang et al., 2021; Vincenti et al., 2022). Simultaneously, the second independent correlation framework describes the behavior of PBAPs and fungal spores. Arabitol and Mannitol, commonly used as fungal spore tracers, show a strong co-variance (r = 0.81) indicating a comparable source as metabolic storage molecules in airborne fungal communities (Gonçalves et al., 2021; Rabhi et al., 2024). These sugar alcohols have moderate to large positive relationships with Glucose (r = 0.61) and Fructose (r = 0.39) suggesting a mixed biogenic source profile of fungal activities, pollen discharge and plant fragments (Gonçalves et al., 2021; Shahid et al., 2025). Arabitol and Mannitol are both weakly or non significantly related with PM10, K^+ and the anhydrosugars suggestive of biogenic emissions independent of seasonal biomass burning sources. Moderate

https://doi.org/10.5194/egusphere-2026-6556
Preprint. Discussion started: 16 November 2026
© Author(s) 2026. CC BY 4.0 License.

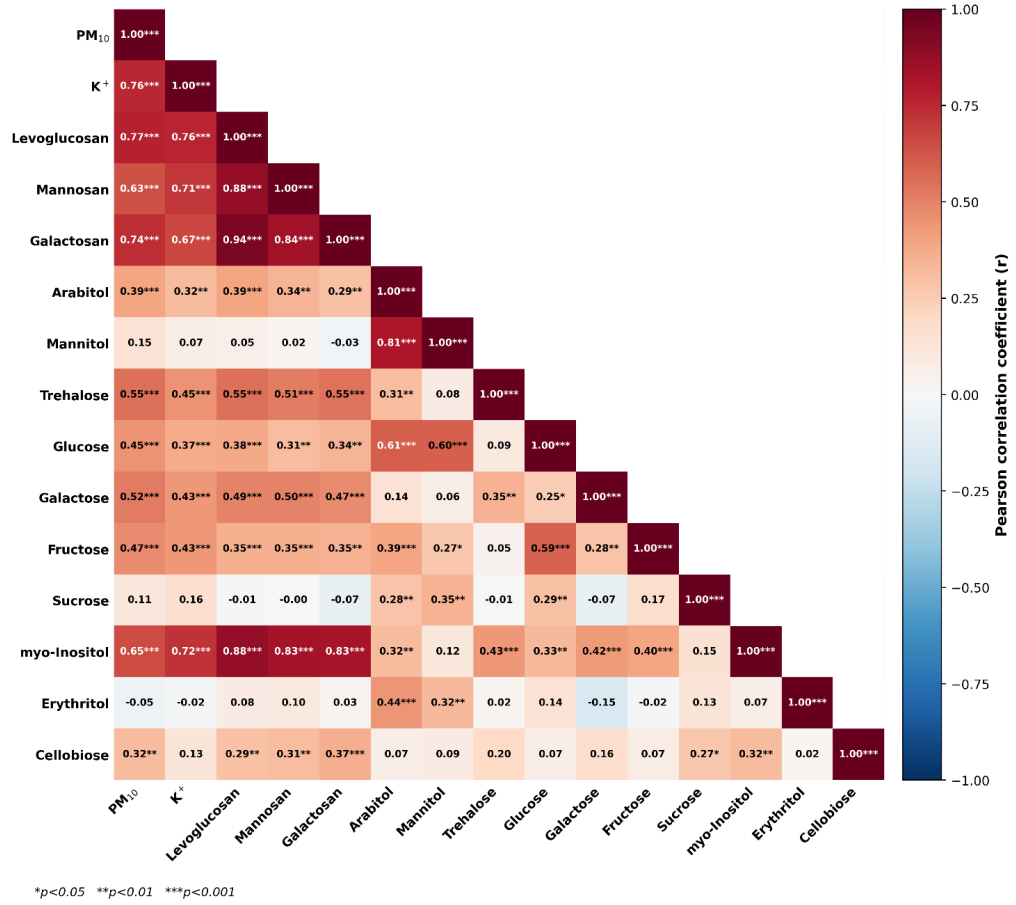


Figure 10 Spearman rank correlation heat map illustrating inter-species relationships among sugar compounds, K^+, and PM10

https://doi.org/10.5194/egusphere-2026-6556
Preprint. Discussion started: 16 November 2026
© Author(s) 2026. CC BY 4.0 License.

and statistically significant correlations were observed between Trehalose and PM10 (r = 0.55) and Levoglucosan (r = 0.55) implying that regional biomass burning events and wind generated dust storms re-suspend top soil particles as well as surface agricultural dust (Nirmalkar et al., 2015a, b). Glucose was closely linked with Fructose (r = 0.59) indicating their co-existence in living plant matter (Fu et al., 2012; Li et al., 2016a). Cellobiose is an intermediate breakdown product of cellulose from mechanical agricultural harvesting and low temperature smoldering and correlates weakly to moderately with the anhydrous sugars (r = 0.29 to 0.37) (Wang et al., 2021; Michalski and Kończyk, 2024). Finally, Sucrose (r = 0.11 with PM10) and Erythritol (r = 0.44 with Arabitol) demonstrate independent behavior in most categories, suggesting of highly specialized or confined seasonal emission events, e.g. localized pollen or microbial blooms rather than massive regional inputs (Nirmalkar et al., 2015a).

3.7 Principal Component Analysis (PCA)

The biplot displays the distribution of the samples and the variable loading vectors along the first two principal components that account for 57.8 % of the total variance (PC1= 38.9 %, and PC2 = 18.9 %). Figure 11 displays that the principal component space clearly distinguishes geochemical clusters and seasonal segregation of the samples. The Autumn and Winter samples are a broad group in the positive quadrant of PC1 with strong and tight loading vectors for anhydrosugars namely Levoglucosan, Mannosan and Galactosan together with Myo-Inositol, Galactose, Trehalose and Cellobiose. The alignment along PC1 is due to the dominant pyrolytic origin, which is driven by the intense agricultural biomass burning (rice straw harvesting in autumn) and residential wood combustion or heating in winter (Li et al., 2021; Vincenti et al., 2022). Myo-Inositol and Trehalose are co-emitted or thermally volatilized with pyrolytic anhydrosugars (Nirmalkar et al., 2015b).

However, samples of Summer constitute a separate cluster in the upper left quadrant with positive loadings on PC2 and negative loadings on PC1. This orientation is in good

https://doi.org/10.5194/egusphere-2026-6556
Preprint. Discussion started: 16 November 2026
© Author(s) 2026. CC BY 4.0 License.

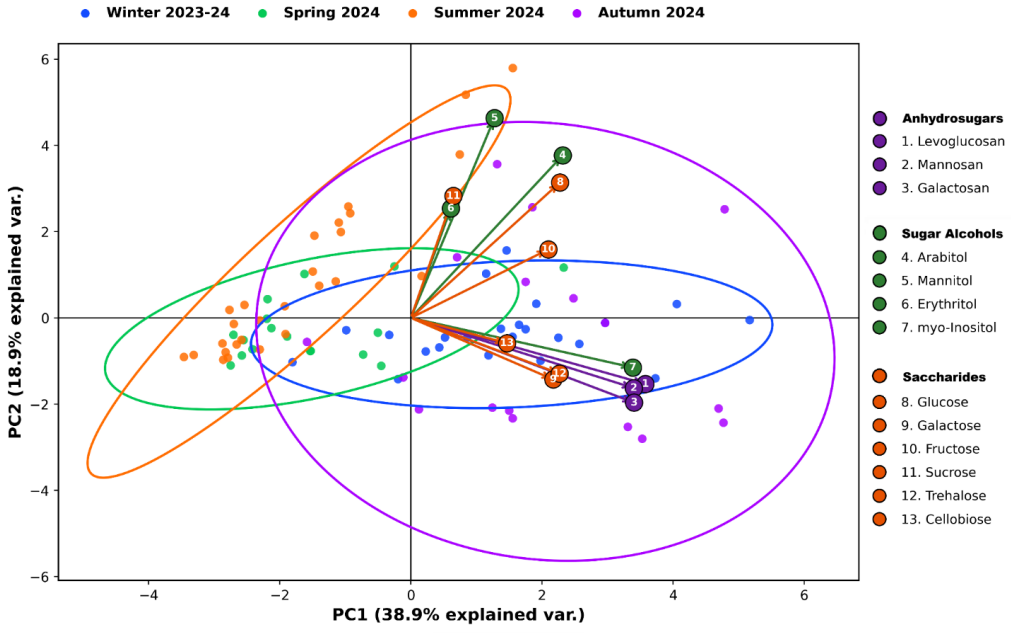


Figure 11 PCA biplot showing key source profiles and variable loadings for sugar compounds in PM10

https://doi.org/10.5194/egusphere-2026-6556
Preprint. Discussion started: 16 November 2026
© Author(s) 2026. CC BY 4.0 License.

alignment with the vectors of fungal spore tracers such as Mannitol, Arabitol, Sucrose, Glucose, and Fructose. The high positive PC2 projection of Mannitol and Arabitol indicates increased biogenic activity, active fungal sporulation, and vegetation metabolic activities during the warm and humid summer monsoon (Pietrogrande et al., 2014; Emygdio et al., 2018; Ramteke et al., 2025). Spring samples occupy an intermediate position, mostly clustered around the origin, suggesting a transitional geochemical condition with moderate biogenic inputs and muted combustion signals. In general, the PCA biplot reveals a simple seasonal dichotomy of atmospheric sugar composition over Faisalabad: a pyrolytic and soil resuspension regime dominant in Autumn and Winter (PC1 driver) and an active biogenic or fungal sporulation regime that governs the summer months (PC2 driver).

3.8 Diagnostic Ratios of Tracer Compounds

Figure 12 depicts diagnostic scatter plot showing association with Levoglucosan/Mannosan and Levoglucosan/K+ and distinct combustion signatures in different seasons in Faisalabad. In all four seasons most data points are in the upper left quadrant labeled “Crop residuals & US-Grass” (Levoglucosan/Mannosan > 10 and Levoglucosan/K+ < 1.0). Levoglucosan/Mannosan concentrations were generally high throughout the year with seasonal averages of 34 ± 8, 26 ± 7, 40 ± 35, 19 ± 22 in Autumn, Winter, Spring, and Summer respectively. Distinctive markers for agricultural wastes including rice straw, wheat straw, and herbaceous grasses have elevated Levoglucosan/Mannosan ratios (> 25-30) due to their unique hemicellulose structures (Wang et al., 2021; Vincenti et al., 2022; Rabhi et al., 2025). One Winter data point falls in the Hardwood domain (Levoglucosan/Mannosan > 1.0) suggesting localized wood burning for heating during extreme cold spells (Islam et al., 2021; Li et al., 2021). The observed Levoglucosan/K^+ ratios remained low across most samples, averaging 0.27 ± 0.12 in Autumn, 0.24 ± 0.28 in Winter, 0.14 ± 0.07 in Spring, and 0.10 ± 0.04 in Summer. Agricultural residues and crop byproducts are rich in inorganic nutrients including K^+,

https://doi.org/10.5194/egusphere-2026-6556
Preprint. Discussion started: 16 November 2026
© Author(s) 2026. CC BY 4.0 License.

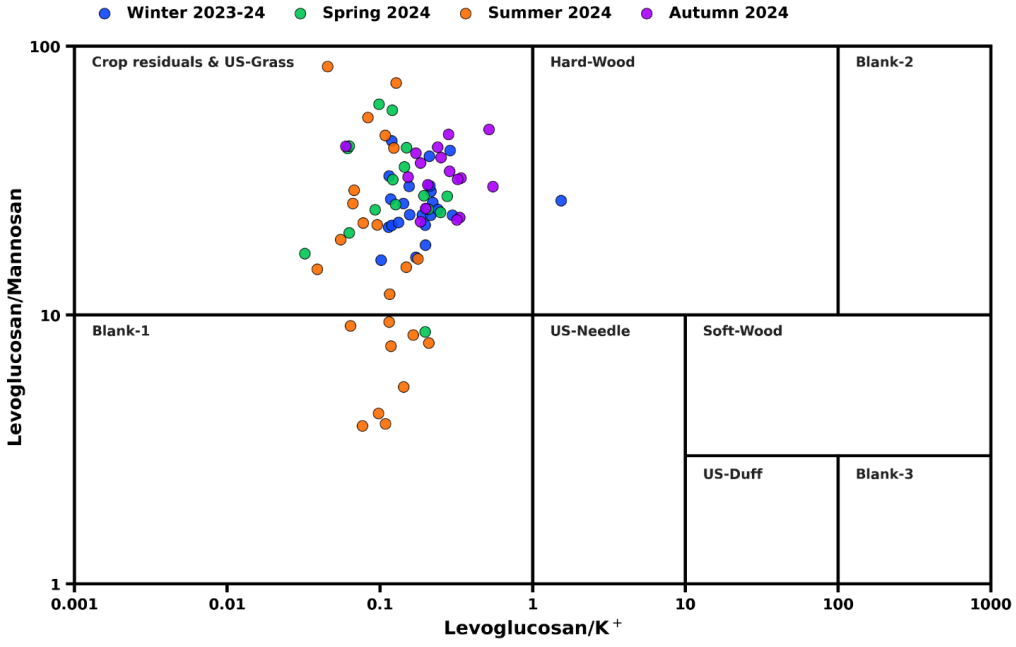


Figure 12 Diagnostic ratios of Levoglucosan/Mannosan and Levoglucosan/K^+ for different biomass combustion sources compared with observed values in the current study.

https://doi.org/10.5194/egusphere-2026-6556
Preprint. Discussion started: 16 November 2026
© Author(s) 2026. CC BY 4.0 License.

resulting in lower Levoglucosan/K^+ ratios compared to burning of forest wood where K^+ is emitted at lower levels than pyrolytic anhydrosugars (Vincenti et al., 2022; Paris et al., 2023). In the Summer samples, variability in the lower range of Levoglucosan/Mannosan is higher. The distribution reveals less open combustion activity, lower total anhydrosugar concentrations and a relative rise in baseline contributions of inorganic dust and biogenic aerosols in warmer months.

3.9 Non-Negative Matrix Factorization (NMF) Analysis

We used a 5 factor Non-Negative Matrix Factorization (NMF) model on the whole data set to identify specific sources of emissions and seasonal changes in particulate organic sugars. During the monitoring campaign, the model was able to distinguish pyrolytic, primary biogenic and soil microbial signatures as demonstrated in Figure 13. The dominant loadings of Factor 1 (Biomass Burning) during the entire study period were Levoglucosan (90 %), Mannosan (75 %) and Galactosan (40 %). These anhydrosugars are the most used molecular markers of biomass burning (Caseiro et al., 2007; Scaramboni et al., 2015; Paris et al. 2023; Wang et al. 2021; Sang et al., 2020) and are obtained by pyrolysis of cellulose and hemicellulose. These compounds accounted for 68.1 % of the total saccharide budget. Also present in the factor was Myo-Inositol (71 %) which is consistent with the fact that sugar alcohols are also released during crop residue and plant material burning (Fu et al. 2010; Tsai et al. 2010; Wang et al. 2021; Vincenti et al. 2022). Factor 2 (Plant Detritus; 10 %) was characterized by Glucose (82 %) and Fructose (43 %). Both are released from developing leaves, flowers, fruits and plant fragments and are abundant in plant materials (Rabhi et al. 2025; Vincenti et al. 2022; Wang et al. 2021). Factor 3 (Soil biota & dust resuspension; 6 %) was characterized by Galactose (79 %) and Trehalose (40 %). Galactose is a soluble carbohydrate found in the tissues of vascular plants, developing leaves, bark, fruit fragments and flower buds (Wang et al. 2021; Rabhi et al. 2025). Wind, crop harvesting and plant senescence mechanically abrade leaves, releasing free galactose to the ambient air (Wang et

https://doi.org/10.5194/egusphere-2026-6556
Preprint. Discussion started: 16 November 2026
© Author(s) 2026. CC BY 4.0 License.

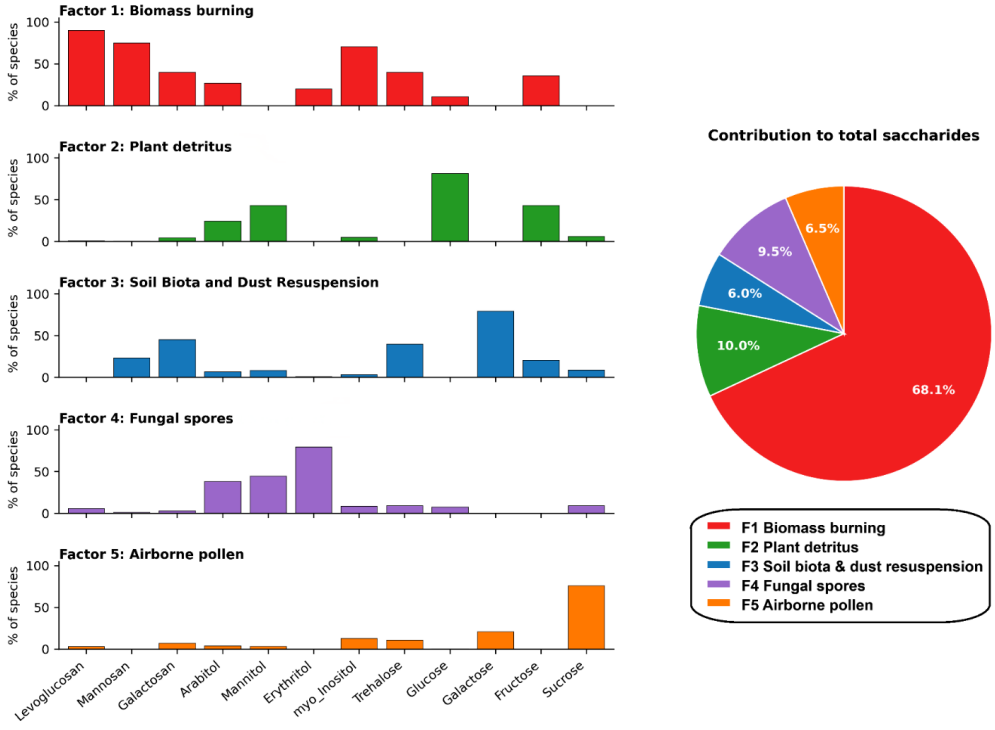


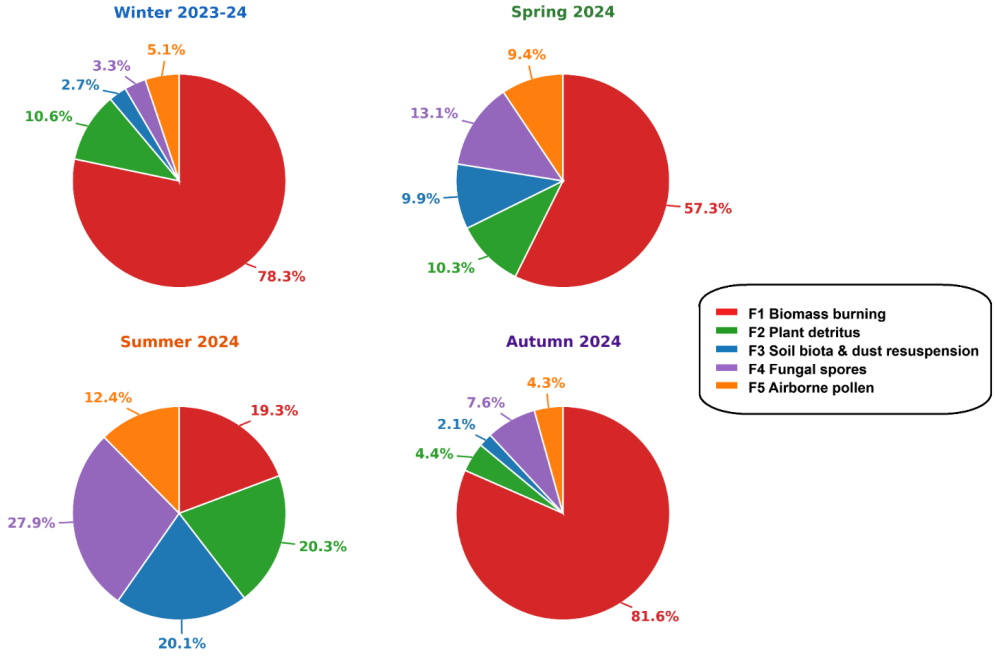
Figure 13 (Left) NMF factor profiles, shown as the percentage of each saccharide apportioned to each of the five factors, and (Right) the contribution of each factor to the total mass of the twelve saccharides.

https://doi.org/10.5194/egusphere-2026-6556
Preprint. Discussion started: 16 November 2026
© Author(s) 2026. CC BY 4.0 License.

al. 2021; Vincenti et al. 2022). Trehalose is a stress protectant and osmoregulator of plants and microorganisms, and is abundant in biologically active surface soils. Trehalose has been suggested as a marker for soil biota and fugitive dust from such soils (Fu et al. 2026; Wang et al 2021). Factor 4 (Fungal spores; 9.5 %) was dominated by Erythritol (79 %), Mannitol (45 %) and Arabitol (38 %). The presence of Arabitol and Mannitol is a commonly utilized marker for airborne fungal spores (Bauer et al. 2008; Wang et al. 2021; Gonçalves et al., 2021). Erythritol (C_4 sugar alcohol) is produced by some microorganisms like airborne fungi, lichens and bacteria (Pietrogrande et al., 2014; Nirmalkar et al., 2015b; Caseiro et al., 2007), which suggests that this factor may be related to other microbial or secondary biogenic sources. Factor 5 (Airborne pollen; 6.5 %), dominated by Sucrose, with small contributions of Galactose, Myo-Inositol and Trehalose. Sucrose is the dominant saccharide in pollen and fragmented pollen grains, and is a major constituent of fine and coarse aerosol during flowering seasons (Michalski and Kończyk 2024; Wang et al. 2021). During flowering seasons, large amounts of fine and coarse particle-bound sucrose are released into the atmosphere by the swelling and the mechanical or osmotic rupture of airborne pollen grains (Fu et al., 2026).

The relative contributions from different sources were seasonally variable, and strongly related to regional agricultural burning cycles and synoptic meteorological variability. The contribution of the five factors varied among seasons (Figure 14). Biomass burning contributed to 81.6 % of saccharide mass in Autumn, 78.3 % in Winter, 57.3 % in Spring and 19.3 % in Summer. The high values in Autumn and Winter are consistent with increased residential heating and cooking, burning of crop residues and shallow stagnant boundary layers, typical of these seasons. Minor secondary inputs were plant detritus (4.4 %-10.6 %), soil biota & dust resuspension (2.1 %-2.7 %), fungal spores (3.3 %-7.6 %) and pollen releases (4.3 %-5.1 %) during Autumn and Winter. In Summer the contribution of biomass burning decreased to 19.3 % and biogenic and soil sources increased, with fungal

https://doi.org/10.5194/egusphere-2026-6556
Preprint. Discussion started: 16 November 2026
© Author(s) 2026. CC BY 4.0 License.



573
574 **Figure 14** Seasonal contributions of the five NMF factors to the total saccharide mass during
575 different seasons.
576

https://doi.org/10.5194/egusphere-2026-6556
Preprint. Discussion started: 16 November 2026
© Author(s) 2026. CC BY 4.0 License.

spores (27.9 %), plant detritus (20.3 %), soil biota & dust resuspension inputs (20.1 %) and pollen (12.4 %) being the most important. The weaker summer contribution of Factor 1 is consistent with stronger vertical mixing, wet scavenging during monsoon and photochemical degradation of Levoglucosan during atmospheric transport (Hennigan et al., 2010) which might lead to an underestimation of biomass burning contribution in summer. Fungal spores increased with the increasing contributions in summer and autumn. Biota from the soil and resuspension of dust input was also highest in Summer and lowest in Autumn and Winter as expected for the hot dry pre-monsoon and monsoon-season conditions that favor the dryness and resuspension of soil. These NMF findings confirm the predominance of primary biogenic aerosols to the ambient sugar profiles during the warm humid season, whereas regional pyrolytic emissions overwhelmingly dominate the particulate saccharide burdens during severe Autumn and Winter haze episodes.

3.10 Regional MODIS Active Fire Occurrence

We combined 72-hour back trajectory clustering with FIRMS MODIS active fire pixel distributions across South Asia to resolve the regional atmospheric transport pathways and transboundary combustion influences affecting Faisalabad in all four seasons. In Autumn (26,660 MODIS fire pixels), the annual peak in levels of biomass burning tracers was dominated by extensive post-harvest burning of rice paddy straw across the agricultural belts of the Indo-Gangetic Plain (IGP) as shown in Figure 15. Cluster 1 (81.2 % occurrence) had a strong influence on the synoptic airflow that crossed the northern and northwestern agricultural belts bringing along high concentrations of Levoglucosan (3220 ng m^{-3}). Meanwhile, even higher mean Levoglucosan loadings were recorded for longer range western trajectories in Cluster 2 (12.5 %) and for southeasterly flows in Cluster 3 (6.2 %) (3832 ng m^{-3} and 3988 ng m^{-3}, respectively), illustrating that both local smoke accumulation and transboundary transport along active fire belts cause severe autumn haze. Throughout Winter, shallow planetary boundary layers and shorter continental air pathways encouraged regional

https://doi.org/10.5194/egusphere-2026-6556
Preprint. Discussion started: 16 November 2026
© Author(s) 2026. CC BY 4.0 License.

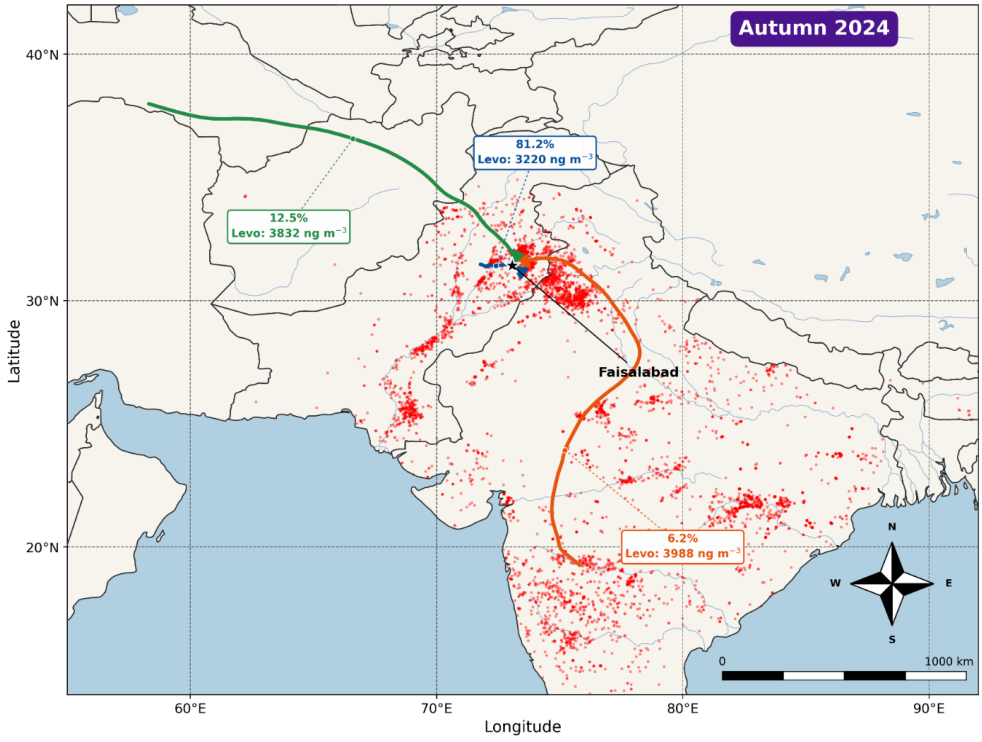


Figure 15 MODIS active fire occurrence overlaid with trajectory associated mean Levoglucosan concentration during Autumn

https://doi.org/10.5194/egusphere-2026-6556
Preprint. Discussion started: 16 November 2026
© Author(s) 2026. CC BY 4.0 License.

atmospheric stagnation (20,093 MODIS fire pixels) as presented in Figure 16. Here, cluster 1 represented the main northwestern pathway (73.9 %; Levo: 2361 ng m^{-3}) whereas slower long-range air masses in cluster 2 (13.0 %; Levo: 2999 ng m^{-3}) and southeasterly trajectories in cluster 3 (13.0 %; Levo: 3368 ng m^{-3}) accumulated larger amounts of tracer due to longer residence times over combustion hot spots. Conversely, organic tracer concentrations decreased significantly during Spring (17,451 MODIS fire pixels) and Summer (15,827 MODIS fire pixels) as regional open fires subsided and atmospheric dispersion increased as shown in Figure 17 and 18. In spring, Cluster 1 (70.6 %) was dominated by northwestern continental air masses (Levo: 903 ng m^{-3}) with secondary contributions from Cluster 2 (23.5 %; Levo: 814 ng m^{-3}) and Cluster 3 (5.9 %; Levo: 778 ng m^{-3}). During Summer, monsoon circulation transported clean, long-range marine air from the Arabian Sea via Cluster 3 (21.7 %; Levo: 580 ng m^{-3}) as well as easterly flows in Cluster 2 (39.1 %; Levo: 246 ng m^{-3}) and northwesterly vectors in Cluster 1 (39.1 %; Levo: 475 ng m^{-3}). During this period, the higher mixing heights and wet deposition effectively suppressed the Levoglucosan concentrations to the annual minimum. Overall, these trajectory dynamics confirm that the primary drivers of elevated Levoglucosan in Faisalabad are transboundary crop burning and winter boundary layer entrapment along major regional air corridors.

https://doi.org/10.5194/egusphere-2026-6556
Preprint. Discussion started: 16 November 2026
© Author(s) 2026. CC BY 4.0 License.

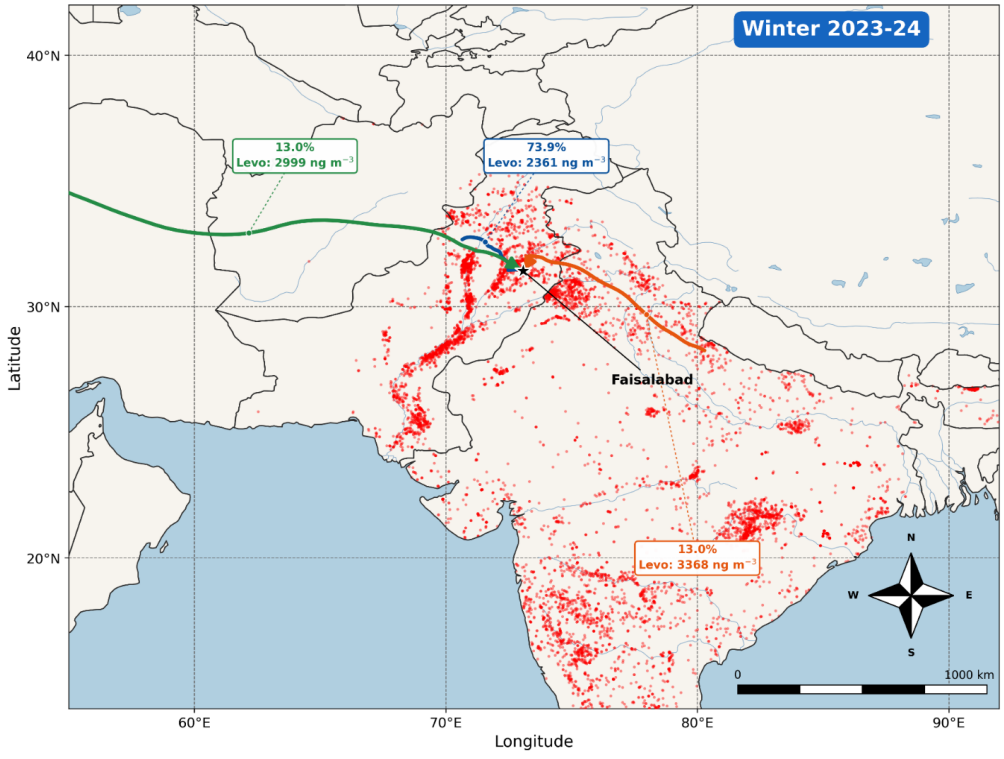


Figure 16 MODIS active fire occurrence overlaid with trajectory associated mean Levoglucosan concentration during Winter

https://doi.org/10.5194/egusphere-2026-6556
Preprint. Discussion started: 16 November 2026
© Author(s) 2026. CC BY 4.0 License.

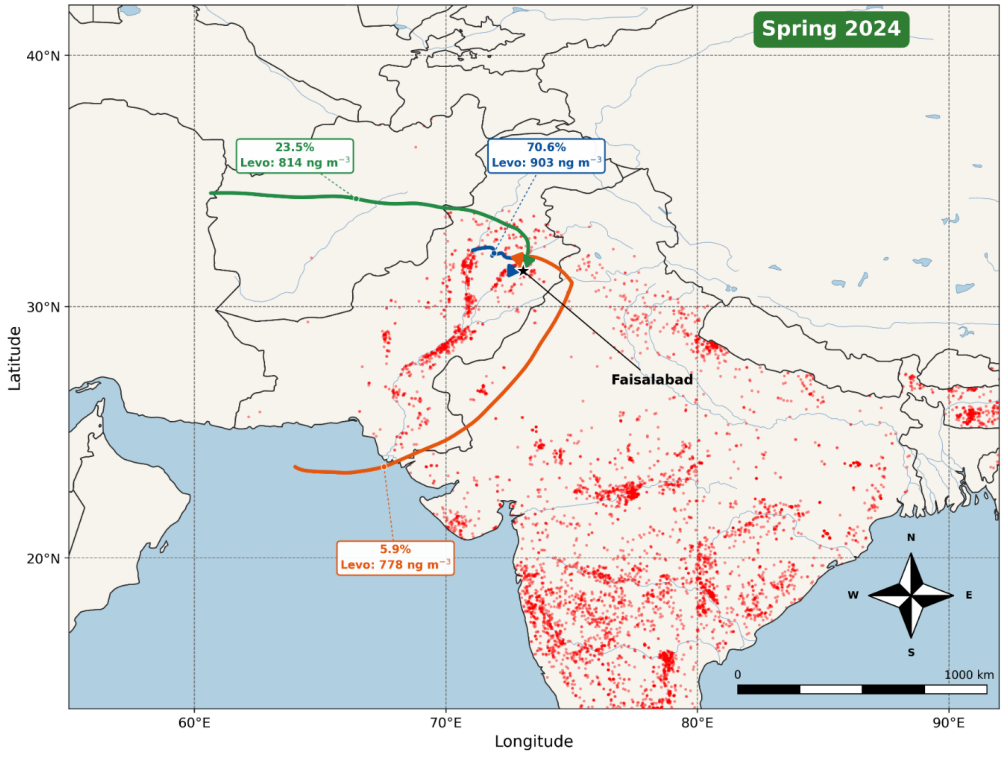


Figure 17 MODIS active fire occurrence overlaid with trajectory associated mean Levoglucosan concentration during Spring

https://doi.org/10.5194/egusphere-2026-6556
Preprint. Discussion started: 16 November 2026
© Author(s) 2026. CC BY 4.0 License.

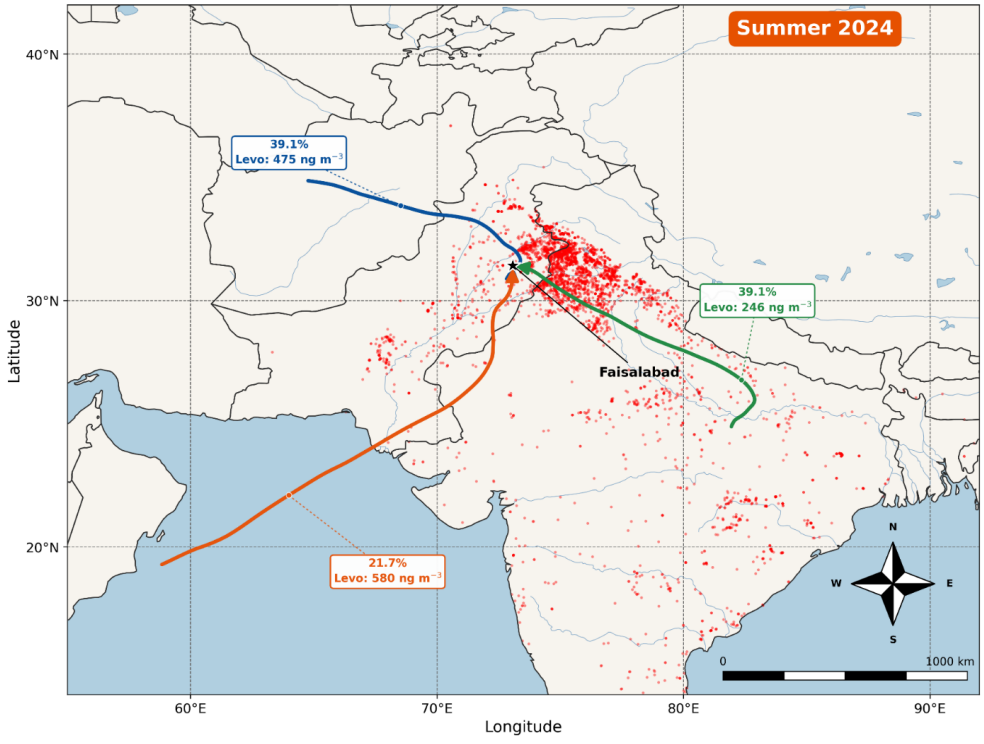


Figure 18 MODIS active fire occurrence overlaid with trajectory associated mean Levoglucosan concentration during Summer

https://doi.org/10.5194/egusphere-2026-6556
Preprint. Discussion started: 16 November 2026
© Author(s) 2026. CC BY 4.0 License.

Conclusion

This study provides a detailed characterization of the year-round particulate matter (PM10) mass, primary organic tracer speciation (sugars, anhydrosugars, sugar alcohols) and synoptic transport pathways over Faisalabad, an agro-industrial hub in central Pakistan. The annual mean PM10 concentration was 658 ± 304 µg m^{-3} (range 169-1177 µg m^{-3}) which was up to 6.3 times higher than the Pak-EPA 24-h standard (150 µg m^{-3}) and 13 times higher than the WHO daily guideline (50 µg m^{-3}). Particulate loadings exhibited severe seasonal variability: Autumn (940 ± 167 µg m^{-3}) > Winter (853 ± 183 µg m^{-3}) > Spring (510 ± 257 µg m^{-3}) > Summer (399 ± 192 µg m^{-3}). The annual mean PM10 (658 ± 304 µg m^{-3}) is similar to historically severe pollution hot spots in Pakistan such as Nazria Pakistan Square, Faisalabad (800 µg m^{-3}), Peshawar (638 µg m^{-3}) and Quetta (700 µg m^{-3}) and regional Indo-Gangetic Plain (IGP) megacities such as Delhi (826 µg m^{-3}) and Bharatpur, India (638 µg m^{-3}). In comparison, these levels are much higher than the annual averages reported in East Asian cities (e.g. Beijing (200 µg m^{-3}) or European sites (23 µg m^{-3})), identifying central Pakistan as one of the world's most particle polluted basins. Chemical speciation showed anhydrosugars accounted for 72 % of total quantified sugar mass. Levoglucosan (3283 ± 1334 ng m^{-3} in Autumn; 2530 ± 964 ng m^{-3} in Winter), Mannosan (101 ± 47 ng m^{-3}) and Galactosan (87 ± 44 ng m^{-3}) were the most abundant species. The rest of the organic sugar fraction was made up of Primary saccharides (17 %, mainly Glucose and Sucrose) and Sugar Alcohols (11 %, mainly Arabitol and Mannitol), with their peaks in relative shares in Summer (34 % and 25.7 %, respectively). The annual mean Levoglucosan concentration (1668 ± 1438 ng m^{-3}) and Autumn peak (3283 ± 1334 ng m^{-3}) are consistent with high post-harvest agricultural burning signatures reported in Lumbini, Nepal (3747 ± 1106 ng m^{-3}), Mahanadi Riverside Basin, India (3250 ng m^{-3}), and Raipur, Central India (2210 ± 2381 ng m^{-3}), and are higher than urban winter levels in New Delhi (1977 ± 971 ng m^{-3}), Xi'an, China (576 ± 99 ng m^{-3}), and

https://doi.org/10.5194/egusphere-2026-6556
Preprint. Discussion started: 16 November 2026
© Author(s) 2026. CC BY 4.0 License.

Krakow, Poland (1950 ng m^{-3}). Fungal spore markers (Mannitol up to 425 ng m^{-3}; Arabitol up to 229 ng m^{-3}) and primary sugars (Glucose up to 540 ng m^{-3}) peaked during summer indicative of high seasonal biological activity similar to agricultural regions of Central India (Nirmalkar et al., 2015b) and North China Plain (Li et al., 2014).

The integrated geochemical, statistical and air mass trajectory framework shows a distinct seasonal dichotomy controlling the organic aerosol regime over central Pakistan. The anhydrosugars represented 81.1 % (Autumn) and 76.2 % (Winter) of total sugars and showed a high co-variance with PM10 (r = 0.77) and inorganic potassium K^+ (r = 0.76). High Levoglucosan/Mannosan (L/M = 26-34) and low Levoglucosan/K^+ (L/K^+ = 0.24-0.27) diagnostic tracer ratios indicate that the main source of Autumn organic carbon loading is open combustion of agricultural crop residues (mainly rice straw). In Winter, pyrogenic inputs continue from crop residue burning, domestic wood heating and biomass fired brick kilns which are severely worsened by shallow planetary boundary layer (PBL) heights and thermal inversions that trap emissions near the surface. As open burning diminishes and temperatures increase, anhydrosugars attain a seasonal minimum (40.3 % in Summer; Levoglucosan = 386 ± 207 ng m^{-3}). PCA and correlation matrices show an independent biogenic mode (PC2 = 18.9 % variance) driven by active fungal sporulation (Arabitol and Mannitol; r = 0.81), plant metabolic activity and wind-driven soil and crustal resuspension during agricultural tilling and wheat harvesting. Summer deep convective mixing and monsoonal wet deposition further reduce regional combustion plumes. Non-negative matrix factorization of twelve saccharides identified five sources: biomass burning (68.1 %), plant detritus (10.0 %), fungal spores (9.5 %), airborne pollen (6.5 %) and soil biota and dust resuspension (6.0 %). Biomass burning was the main source of saccharide mass in autumn (82 %) and winter (78 %), while biogenic sources contributed 81 % to the saccharide mass in summer due to the strong decrease of biomass burning. MODIS active fire distribution

https://doi.org/10.5194/egusphere-2026-6556
Preprint. Discussion started: 16 November 2026
© Author(s) 2026. CC BY 4.0 License.

(20,093-26,660 pixels in Winter and Autumn) and CWT modeling indicates that severe CWT loadings (700-900 µg m^{-3}) are associated with long range and transboundary IGP trajectories. This confirms that the seasonal haze crisis is predominantly caused by regional agricultural biomass combustion that is common across the IGP, compared to western arid mineral dust inflows (300-500 µg m^{-3}).

Atmospheric Policy and Climate Implications

The above mentioned empirical insights reveal critical implications for atmospheric chemistry, regional air quality management, and climate policy across South Asia. The extreme abundance of anhydrosugars highlights cellulose pyrolytic breakdown as the single most critical driver of aerosol organic carbon during cold seasons. Global and regional chemistry transport models must account for these seasonal, high-intensity pyrogenic surges to accurately simulate regional aerosol radiative forcing and cloud condensation nuclei (CCN) formation. Because 73 % of back trajectories represent stagnant or regional continental pathways crossing agricultural belts, local municipal emission controls alone will not solve the Autumn and Winter smog crisis. Addressing regional haze in central Pakistan requires regional interventions, and coordinated cross border air quality management frameworks across the Indo-Gangetic Plain, specifically targeting agricultural mechanization (e.g., happy seeder adoption), crop residue management alternatives, modernizing brick kiln technologies, and alternatives to domestic biomass heating. To control warm season coarse particles, unpaved road stabilization, urban greening and dust suppression strategies are required.

Limitations

There are certain limitations which should be considered when evaluating these findings. Sampling was conducted at a single urban and industrial receptor site in Faisalabad.

https://doi.org/10.5194/egusphere-2026-6556
Preprint. Discussion started: 16 November 2026
© Author(s) 2026. CC BY 4.0 License.

While trajectory analysis confirms strong regional representation, micro scale urban street canyon effects and local road dust resuspension may influence specific primary sugar proportions. Levoglucosan and other sugar compounds can undergo atmospheric degradation via reactions with hydroxyl (OH) radicals during long range transport, potentially altering diagnostic ratios (Levoglucosan/Mannosan) and (Levoglucosan/K^+) under intense photochemical conditions. Satellite MODIS fire counts capture open field agricultural burning but undercount low temperature smoldering and indoor domestic heating and cooking, which contribute to cold season anhydrosugar loadings. Future studies should integrate multi-site vertical profiling, photochemical aging kinetics, and high resolution local emission inventories to refine source contribution estimates.

Data Availability

The data underlying this study (NMF input matrix, air mass trajectory outputs, and MODIS fire data) are available at Zenodo (https://doi.org/10.5281/zenodo.23600261) (Alvi et al., 2026). MODIS active fire data and air mass trajectory outputs can also be directly accessed from NASA FIRMS (https://earthdata.nasa.gov/firms), and HYSPLIT trajectories were computed with NOAA's READY system (https://www.ready.noaa.gov/HYSPLIT.php).

Declaration

The authors declare no conflicts of interest.

Acknowledgements

The authors are thankful to the Institute for Chemical Technologies and Analytics, Vienna University of Technology (TU-Wien), Austria for providing technical assistance.

Ethical Approval

The manuscript is not submitted to any other journal for simultaneous consideration, and submitted only to "Atmospheric Chemistry and Physics". The submitted work is original and never have been published elsewhere in any form or language. This study has not been

https://doi.org/10.5194/egusphere-2026-6556
Preprint. Discussion started: 16 November 2026
© Author(s) 2026. CC BY 4.0 License.

reported as split up work into several parts to increase the quantity of submissions and never been submitted to various journals or to one journal over time. Results are presented clearly, honestly, and without fabrication, falsification or inappropriate data manipulation including the provided images.

Consent to Participate

This work does not involve any experiment on persons/ patients/ study participants so, consent to participate is not applicable and not required for this work.

Consent to Publish

This work does not involve any experiment on persons/ patients/ study participants so, consent to publish is not applicable and not required for this work.

Authors Contributions

All authors contributed to the study conception and design. Material preparation, data collection and analysis were performed by Muhammad Usman Alvi. Discussion about sources was conducted by Junaid Anwer, and some statistical calculations were conducted by Farhan Anwer. The first draft of the manuscript was written by Muhammad Usman Alvi. All authors read and approved the final manuscript.

Funding

The authors declare that no funds, grants, or other support was received during the preparation of this manuscript.

Competing Interests

The authors have no relevant financial or non-financial interests to disclose.

Abbreviations

Arab	Arabitol
AGL	Above Ground Level

https://doi.org/10.5194/egusphere-2026-6556
Preprint. Discussion started: 16 November 2026
© Author(s) 2026. CC BY 4.0 License.

CCN	Cloud Condensation Nuclei
COPD	Chronic Obstructive Pulmonary Disease
CPEC	China Pakistan Economic Corridor
CWT	Concentration Weighted Trajectory
DL	Detection Limit
Eryt	Erythritol
FIRMS	Fire Information for Resource Management System
Fruc	Fructose
Galn	Galactosan
Gals	Galactose
GDAS	Global Data Assimilation System
GDP	Gross Domestic Product
Gluc	Glucose
HPAEC-PAD	High Performance Anion Exchange Chromatography with Pulsed Amperometric Detection
HYSPLIT	Hybrid Single Particle Lagrangian Integrated
IGP	Indo Gangetic Plain
Inos	Inositol
Levo	Levoglucosan
Mans	Mannosan
Mant	Mannitol
MDL	Method Detection Limit
MODIS	Moderate Resolution Imaging Spectroradiometer
MSA	Methane Sulfonic Acid
NAAQS	National Ambient Air Quality Standards

https://doi.org/10.5194/egusphere-2026-6556
Preprint. Discussion started: 16 November 2026
© Author(s) 2026. CC BY 4.0 License.

NASA	National Aeronautics and Space Administration
NEQS	National Environmental Quality Standards
NMF	Non-negative Matrix Factorization
NOAA	National Oceanic and Atmospheric Administration
Pak-EPA	Pakistan Environmental Protection Agency
PBAPs	Primary Biogenic Aerosol Particles
PBL	Planetary Boundary Layer
PCA	Principal Component Analysis
PCAP	Pakistan Clean Air Program
PM	Particulate Matter
Sucr	Sucrose
Treh	Trehalose
USEPA	United States Environmental Protection Agency
WHO	World Health Organization

https://doi.org/10.5194/egusphere-2026-6556
Preprint. Discussion started: 16 November 2026
© Author(s) 2026. CC BY 4.0 License.

References

Adam, M. G., Tran, P. T., Bolan, N., and Balasubramanian, R.: Biomass burning-derived airborne particulate matter in Southeast Asia: a critical review, J. Hazard. Mater., 407, 124760, https://doi.org/10.1016/j.jhazmat.2020.124760, 2021.

Adrees, M., Ibrahim, M., Shah, A. M., Abbas, F., Saleem, F., Rizwan, M., Hina, S., Jabeen, F., and Ali, S.: Gaseous pollutants from brick kiln industry decreased the growth, photosynthesis, and yield of wheat (Triticum aestivum L.), Environ. Monit. Assess., 188, 267, https://doi.org/10.1007/s10661-016-5273-8, 2016.

Aggarwal, S. G. and Kawamura, K.: Carbonaceous and inorganic composition in long-range transported aerosols over northern Japan: implication for aging of water-soluble organic fraction, Atmos. Environ., 43, 2532–2540, https://doi.org/10.1016/j.atmosenv.2009.02.032, 2009.

Ahmad, I., Khan, B., Khan, S., Rahman, Z., Khan, M. A., and Gul, N.: Airborne PM10 and lead concentrations at selected traffic junctions in Khyber Pakhtunkhwa, Pakistan: implications for human health, Atmos. Pollut. Res., 10, 1320–1325, https://doi.org/10.1016/j.apr.2019.03.003, 2019.

Ahmad, S., Zeb, B., Ditta, A., Alam, K., Ahmad, I., and Usman, F.: Seasonal variations of particulate matter in two size fractions (PM2.5 and PM10) and their relationship with meteorological parameters in Lahore, Pakistan, Environ. Sci.: Adv., 4, 1103–1116, https://doi.org/10.1039/d5va00004a, 2025.

Allabakash, S., Lim, S., Chong, K. S., and Yamada, T. J.: Particulate matter concentrations over South Korea: impact of meteorology and other pollutants, Remote Sens., 14, 4849, https://doi.org/10.3390/rs14194849, 2022.

Alnagran, H., Mansour, H., Alashrah, S., Suardi, N., and Rahman, A. A.: Evaluation of toxic heavy metals and health risk in airborne particulate matter at Qassim region, Saudi Arabia, Trends Sci., 20, 6978, https://doi.org/10.48048/tis.2023.6978, 2023.

Alvi, M. U., Chishtie, F., Shahid, I., Mahmud, T., and Hussain, R.: Traffic- and industry-related air pollution exposure assessment in an Asian megacity, CLEAN – Soil Air Water, 46, 1600773, https://doi.org/10.1002/clen.201600773, 2018.

Alvi, M. U., Anwer, J., Anwer, F.: Measurement Report: PM10-Bound Organic Molecular Tracers (Saccharides) from an Agro-Industrial Metropolis in the Indo-Gangetic Plain (IGP): Seasonal Variations and Source Attribution (Paper Data), Zenodo, https://doi.org/10.5281/zenodo.23600261, 2026.

Amarloei, A., Fazlzadeh, M., Jafari, A. J., Zarei, A., and Mazloomi, S.: Particulate matters and bioaerosols during Middle East dust storms events in Ilam, Iran, Microchem. J., 152, 104280, https://doi.org/10.1016/j.microc.2019.104280, 2020.

Andreae, M. O. and Rosenfeld, D.: Aerosol–cloud–precipitation interactions. Part 1. The nature and sources of cloud-active aerosols, Earth-Sci. Rev., 89, 13–41, https://doi.org/10.1016/j.earscirev.2008.03.001, 2008.

https://doi.org/10.5194/egusphere-2026-6556
Preprint. Discussion started: 16 November 2026
© Author(s) 2026. CC BY 4.0 License.



Ankit, Y., Wolkenstein, K., and Dietze, E.: Fingerprinting biomass burning tracers: isomer-specific profiling of monosaccharide anhydrides using LC-MS/MS and GC–MS, Org. Geochem., 105177, https://doi.org/10.1016/j.orggeochem.2026.105177, 2026.

Arif, M. and Parveen, S.: Spatial and temporal variation of airborne particulate matter (PM2.5 and PM10) and associated human health risk in urban microenvironments, Environ. Monit. Arif, M. and Parveen, S.: Carcinogenic effects of indoor black carbon and particulate matters (PM2.5 and PM10) in rural households of India, Environ. Sci. Pollut. Res., 28, 2082–2096, https://doi.org/10.1007/s11356-020-10668-5, 2021.

Ashraf, M. F., Ahmad, R. U., and Tareen, H. K.: Worsening situation of smog in Pakistan: a tale of three cities, Ann. Med. Surg., 79, 103947, https://doi.org/10.1016/j.amsu.2022.103947, 2022.

Aslam, A., Ibrahim, M., Shahid, I., Mahmood, A., Irshad, M. K., Yamin, M., Ghazala, Tariq, M., and Shamshiri, R. R.: Pollution characteristics of particulate matter (PM2.5 and PM10) and constituent carbonaceous aerosols in a South Asian future megacity, Appl. Sci., 10, 8864, https://doi.org/10.3390/app10248864, 2020.

Aziz, A. and Bajwa, I. U.: Energy and pollution control opportunities for Lahore, in: Urban Transport X, edited by: Brebbia, C. A. and Wadhwa, L. C., WIT Press, Southampton, UK, 751–760, https://www.witpress.com/elibrary/wit-transactions-on-the-built-environment/75/12203, 2004.

Bauer, H., Claeys, M., Vermeylen, R., Schueller, E., Weinke, G., Berger, A., and Puxbaum, H.: Arabitol and mannitol as tracers for the quantification of airborne fungal spores, Atmos. Environ., 42, 588–593, https://doi.org/10.1016/j.atmosenv.2007.10.013, 2008.

Begum, B. A., Paul, S. K., Dildar Hossain, M., Biswas, S. K., and Hopke, P. K.: Indoor air pollution from particulate matter emissions in different households in rural areas of Bangladesh, Build. Environ., 44, 898–903, https://doi.org/10.1016/j.buildenv.2008.06.005, 2009.

Bhattarai, H., Saikawa, E., Wan, X., Zhu, H., Ram, K., Gao, S., Kang, S., Zhang, Q., Zhang, Y., Wu, G., Wang, X., Kawamura, K., Fu, P., and Cong, Z.: Levoglucosan as a tracer of biomass burning: recent progress and perspectives, Atmos. Res., 220, 20–33, https://doi.org/10.1016/j.atmosres.2019.01.004, 2019.

Bhuyan, P., Deka, P., Prakash, A., Balachandran, S., and Hoque, R. R.: Chemical characterization and source apportionment of aerosol over mid Brahmaputra Valley, India, Environ. Pollut., 234, 997–1010, https://doi.org/10.1016/j.envpol.2017.12.009, 2018.

Biswas, K. F., Ghauri, B. M., and Husain, L.: Gaseous and aerosol pollutants during fog and clear episodes in South Asian urban atmosphere, Atmos. Environ., 42, 7775–7785, https://doi.org/10.1016/j.atmosenv.2008.04.056, 2008.

Budhavant, K. B., Rao, P. S., Safai, P. D., and Ali, K.: Chemistry of monsoon and post-monsoon rains at a high altitude location, Sinhagad, India, Aerosol Air Qual. Res., 9, 65–79, https://doi.org/10.4209/aaqr.2008.07.0033, 2009.

https://doi.org/10.5194/egusphere-2026-6556
Preprint. Discussion started: 16 November 2026
© Author(s) 2026. CC BY 4.0 License.

Bulbul, G., Shahid, I., Chishtie, F., Shahid, M. Z., Hundal, R. A., Zahra, F., and Shahzad, M. I.: PM10 sampling and AOD trends during 2016 winter fog season in the Islamabad region, Aerosol Air Qual. Res., 18, 188–199, https://doi.org/10.4209/aaqr.2017.01.0014, 2018.

Bureau of Statistics: 2026 Statistical pocket book of the Punjab, Planning & Development Board, Government of the Punjab, https://bos.punjab.gov.pk/statistical_pocket_book (last access: 30 September 2026), 2026.

Burnett, R., Chen, H., Szyszkowicz, M., Fann, N., Hubbell, B., Pope, C. A., Apte, J. S., Brauer, M., Cohen, A., Weichenthal, S., Coggins, J., Di, Q., Brunekreef, B., Frostad, J., Lim, S. S., Kan, H., Walker, K. D., Thurston, G. D., Hayes, R. B., Lim, C. C., Turner, M. C., Jerrett, M., Krewski, D., Gapstur, S. M., Diver, W. R., Ostro, B., Goldberg, D., Crouse, D. L., Martin, R. V., Peters, P., Pinault, L., Tjepkema, M., van Donkelaar, A., Villeneuve, P. J., Miller, A. B., Yin, P., Zhou, M., Wang, L., Janssen, N. A. H., Marra, M., Atkinson, R. W., Tsang, H., Quoc Thach, T., Cannon, J. B., Allen, R. T., Hart, J. E., Laden, F., Cesaroni, G., Forastiere, F., Weinmayr, G., Jaensch, A., Nagel, G., Concin, H., and Spadaro, J. V.: Global estimates of mortality associated with long-term exposure to outdoor fine particulate matter, P. Natl. Acad. Sci. USA, 115, 9592–9597, https://doi.org/10.1073/pnas.1803222115, 2018.

Caseiro, A., Marr, I. L., Claeys, M., Kasper-Giebl, A., Puxbaum, H., and Pio, C. A.: Determination of saccharides in atmospheric aerosol using anion-exchange high-performance liquid chromatography and pulsed-amperometric detection, J. Chromatogr. A, 1171, 37–45, https://doi.org/10.1016/j.chroma.2007.09.038, 2007.

Chakraborty, A. and Gupta, T.: Chemical characterization and source apportionment of submicron (PM1) aerosol in Kanpur region, India, Aerosol Air Qual. Res., 10, 433–445, https://doi.org/10.4209/aaqr.2009.11.0071, 2010.

Chen, F., Zhang, X., Zhu, X., Zhang, H., Gao, J., and Hopke, P. K.: Chemical characteristics of PM2.5 during a 2016 winter haze episode in Shijiazhuang, China, Aerosol Air Qual. Res., 17, 368–380, https://doi.org/10.4209/aaqr.2016.06.0274, 2017.

Chen, H. Y. and Liu, T. W.: Composition and biogeochemical effects of carbohydrates in aerosols in coastal environment, J. Mar. Sci. Eng., 12, 1834, https://doi.org/10.3390/jmse12101834, 2024.

Cheng, Y., Engling, G., He, K. B., Duan, F. K., Ma, Y. L., Du, Z. Y., Liu, J. M., Zheng, M., and Weber, R. J.: Biomass burning contribution to Beijing aerosol, Atmos. Chem. Phys., 13, 7765–7781, https://doi.org/10.5194/acp-13-7765-2013, 2013.

Choi, N. R., Lee, S. P., Lee, J. Y., Jung, C. H., and Kim, Y. P.: Speciation and source identification of organic compounds in PM10 over Seoul, South Korea, Chemosphere, 144, 1589–1596, https://doi.org/10.1016/j.chemosphere.2015.10.041, 2016.

Devi, N. L., Yadav, I. C., and Kumar, A.: Estimation of particulate matter (PM10) over Middle Indo-Gangetic Plain (Patna) of India: seasonal variation and source apportionment, Atmosphere, 15, 878, https://doi.org/10.3390/atmos15080878, 2024.

https://doi.org/10.5194/egusphere-2026-6556
Preprint. Discussion started: 16 November 2026
© Author(s) 2026. CC BY 4.0 License.

Dong, Z., Lv, P., Lu, J., Qian, G., Zhang, Z., and Luo, W.: Geomorphology and origin of Yardangs in the Kumtagh Desert, Northwest China, Geomorphology, 139–140, 145–154, https://doi.org/10.1016/j.geomorph.2011.10.012, 2012.

Emygdio, A. P. M., Andrade, M. F., Gonçalves, F. L. T., Engling, G., Zanetti, R. H. S., and Kumar, P.: Biomarkers as indicators of fungal biomass in the atmosphere of São Paulo, Brazil, Sci. Total Environ., 612, 809–821, https://doi.org/10.1016/j.scitotenv.2017.08.153, 2018.

Engling, G., Lee, J. J., Sie, H. J., Wu, Y. C., and I, Y. P.: Anhydrosugar characteristics in biomass smoke aerosol – case study of environmental influence on particle-size of rice straw burning aerosol, J. Aerosol Sci., 56, 2–14, https://doi.org/10.1016/j.jaerosci.2012.10.001, 2013.

Excise and Taxation Department Punjab: Vehicle registration statistics: District Faisalabad, Office of the Additional Director General, Government of the Punjab, Lahore, https://excise.punjab.gov.pk/pro-active-disclosure (last access: 30 September 2026), 2024.

Farah, W., Nakhlé, M. M., Abboud, M., Ziade, N., Annesi-Maesano, I., Zaarour, R., Saliba, N., Germanos, G., Saliba, N. A., Shihadeh, A. L., and Gerard, J.: Analysis of the continuous measurements of PM10 and PM2.5 concentrations in Beirut, Lebanon, Environ. Eng. Manag. J., 17, 1693–1700, https://doi.org/10.30638/eemj.2018.168, 2018.

Fleury, V., Himsl, R., Joost, S., Nicastro, N., Bereau, M., Guessous, I., and Burkhard, P. R.: Geospatial analysis of individual-based Parkinson's disease data supports a link with air pollution: a case-control study, Parkinsonism Relat. D., 83, 41–48, https://doi.org/10.1016/j.parkreldis.2020.12.013, 2021.

Fu, P. Q. and Kawamura, K.: Diurnal variations of polar organic tracers in summer forest aerosols: a case study of a Quercus and Picea mixed forest in Hokkaido, Japan, Geochem. J., 45, 297–308, https://doi.org/10.2343/geochemj.1.0123, 2011.

Fu, P. Q., Kawamura, K., Pavuluri, C. M., Swaminathan, T., and Chen, J.: Molecular characterization of urban organic aerosol in tropical India: contributions of primary emissions and secondary photooxidation, Atmos. Chem. Phys., 10, 2663–2689, https://doi.org/10.5194/acp-10-2663-2010, 2010.

Fu, P., Kawamura, K., Kobayashi, M., and Simoneit, B. R. T.: Seasonal variations of sugars in atmospheric particulate matter from Gosan, Jeju Island: significant contributions of airborne pollen and Asian dust in spring, Atmos. Environ., 55, 234–239, https://doi.org/10.1016/j.atmosenv.2012.02.061, 2012.

Fu, P., Wan, X., Ren, H., Pan, X., Sun, Y., Wang, Z., Wang, L., Wang, P., Yue, S., Su, H., Cheng, Y., Kawamura, K., and Cong, Z.: Seasonal variations of primary biological and biomass burning aerosols in the central Himalayas, Fundam. Res., 6, 986–993, https://doi.org/10.1016/j.fmre.2024.05.020, 2026.

https://doi.org/10.5194/egusphere-2026-6556
Preprint. Discussion started: 16 November 2026
© Author(s) 2026. CC BY 4.0 License.

Ghauri, B., Lodhi, A., and Mansha, M.: Development of baseline (air quality) data in Pakistan, Environ. Monit. Assess., 127, 237–252, https://doi.org/10.1007/s10661-006-9276-8, 2007.

Gheorghe, I. F. and Ion, B.: The effects of air pollutants on vegetation and the role of vegetation in reducing atmospheric pollution, in: The Impact of Air Pollution on Health, Economy, Environment and Agricultural Sources, edited by: Khallaf, M., InTech, https://doi.org/10.5772/17660, 2011.

Giri, B., Patel, K. S., Jaiswal, N. K., Sharma, S., Ambade, B., Wang, W., Simonich, S. L. M., and Simoneit, B. R. T.: Composition and sources of organic tracers in aerosol particles of industrial central India, Atmos. Res., 312–324, https://doi.org/10.1016/j.atmosres.2012.09.016, 2013.

Gonçalves, C., Rienda, I. C., Pina, N., Gama, C., Nunes, T., Tchepel, O., and Alves, C.: PM10-bound sugars: chemical composition, sources and seasonal variations, Atmosphere, 12, 194, https://doi.org/10.3390/atmos12020194, 2021.

Gulshan, J.-E., Hossain, S. A., Hossain, M. E., Islam, M. M., Emon, S. Z., Manzum, A. A., Jashim, Z. B., Huda, N., and Rahman, M. M.: Seasonal variations of microbes in particulate matter obtained from Dhaka City in Bangladesh, Environ. Pollut. Bioavailab., 33, 122–134, https://doi.org/10.1080/26395940.2021.1940302, 2021.

Gupta, L., Dev, R., Zaidi, K., Sunder Raman, R., Habib, G., and Ghosh, B.: Assessment of PM10 and PM2.5 over Ghaziabad, an industrial city in the Indo-Gangetic Plain: spatio-temporal variability and associated health effects, Environ. Monit. Assess., 193, 735, https://doi.org/10.1007/s10661-021-09411-5, 2021.

Hamidi, M., Ghobadi, T., Shao, Y., Fallah, B., Rostami, M., and Mao, R..: Investigation of the role of southwestern Asia dust events on urban air pollution: a case study of Ahvaz, a highly polluted city, Sci. Rep., 15, 21981, https://doi.org/10.1038/s41598-025-07634-x, 2025.

Hopke, P. K., Al-Hemoud, A., Alahmad, B., and Koutrakis, P.: Characterization and sources of PM10 in Kuwait, Atmos. Environ., 382, 122223, https://doi.org/10.1016/j.atmosenv.2026.122223, 2026.

Huang, R. J., Zhang, Y., Bozzetti, C., Ho, K. F., Cao, J. J., Han, Y., Daellenbach, K. R., Slowik, J. G., Platt, S. M., Canonaco, F., Zotter, P., Wolf, R., Pieber, S. M., Bruns, E. A., Crippa, M., Ciarelli, G., Piazzalunga, A., Schwikowski, M., Abbaszade, G., Schnelle-Kreis, J., Zimmermann, R., An, Z., Szidat, S., Baltensperger, U., El Haddad, I., and Prévôt, A. S. H.: High secondary aerosol contribution to particulate pollution during haze events in China, Nature, 514, 218–222, https://doi.org/10.1038/nature13774, 2014.

Iinuma, Y., Engling, G., Puxbaum, H., and Herrmann, H.: A highly resolved anion-exchange chromatographic method for determination of saccharidic tracers for biomass combustion and primary bio-particles in atmospheric aerosol, Atmos. Environ., 43, 1367–1371, https://doi.org/10.1016/j.atmosenv.2008.11.020, 2009.

https://doi.org/10.5194/egusphere-2026-6556
Preprint. Discussion started: 16 November 2026
© Author(s) 2026. CC BY 4.0 License.

997 Ishtiaq, T., Jamil, N., Masood, Z., Mushtaq, A., and Bazai, Z. A.: Comparative study of air
998 particulate matter concentrations in different traffic stressed sites of Quetta city, with
999 special reference to their harmful impact on human health, Biol. Forum, 7, 357–362,
1000 https://www.researchtrend.net/bfij/bfij_volume-14.php (last access: 30 September
1001 2026), 2015.

1002 Islam, M. R., Jayarathne, T., Simpson, I. J., Werden, B., Maben, J., Gilbert, A., Praveen, P.
1003 S., Adhikari, S., Panday, A. K., Rupakheti, M., Blake, D. R., Yokelson, R. J., DeCarlo,
1004 P. F., Keene, W. C., and Stone, E. A.: Ambient air quality in the Kathmandu Valley,
1005 Nepal, during the pre-monsoon: concentrations and sources of particulate matter and
1006 trace gases, Atmos. Chem. Phys., 20, 2927–2951, https://doi.org/10.5194/acp-20-2927-
1007 2020, 2020.

1008 Islam, M. R., Li, T., Mahata, K., Khanal, N., Werden, B., Giordano, M. R., Praveen, P. S.,
1009 Dhital, N. B., Gurung, A., Panday, A. K., and Joshi, I. B.: Wintertime air quality in
1010 Lumbini, Nepal: sources of fine particle organic carbon, ACS Earth Space Chem., 5,
1011 226–238, https://doi.org/10.1021/acsearthspacechem.0c00269, 2021.

1012 Islam, M. R., Li, T., Mahata, K., Khanal, N., Werden, B., Giordano, M. R., Puppala, S. P.,
1013 Dhital, N. B., Gurung, A., Saikawa, E., Panday, A. K., Yokelson, R. J., DeCarlo, P. F.,
1014 and Stone, E. A.: Wintertime air quality across the Kathmandu Valley, Nepal:
1015 concentration, composition, and sources of fine and coarse particulate matter, ACS
1016 Earth Space Chem., 6, 2955–2971, https://doi.org/10.1021/acsearthspacechem.2c00243,
1017 2022.

1018 Javed, W., Iakovides, M., Stephanou, E. G., Wolfson, J. M., Koutrakis, P., and Guo, B.:
1019 Concentrations of aliphatic and polycyclic aromatic hydrocarbons in ambient PM2.5
1020 and PM10 particulates in Doha, Qatar, J. Air Waste Manage. Assoc., 69, 162–177,
1021 https://doi.org/10.1080/10962247.2018.1520754, 2019.

1022 Jia, Y., Clements, A. L., and Fraser, M. P.: Saccharide composition in atmospheric particulate
1023 matter in the southwest US and estimates of source contributions, J. Aerosol Sci., 41,
1024 62–73, https://doi.org/10.1016/j.jaerosci.2009.08.005, 2010.

1025 Jung, J., Lee, S., Kim, H., Kim, D., Lee, H., and Oh, S.: Quantitative determination of the
1026 biomass-burning contribution to atmospheric carbonaceous aerosols in Daejeon, Korea,
1027 during the rice-harvest period, Atmos. Environ., 89, 642–650,
1028 https://doi.org/10.1016/j.atmosenv.2014.03.010, 2014.

1029 Kampa, M. and Castanas, E.: Human health effects of air pollution, Environ. Pollut., 151,
1030 362–367, https://doi.org/10.1016/j.envpol.2007.06.012, 2008.

1031 Khan, S., Zeb, B., Ullah, S., Huraira, M. M., Ali, G., Zahid, S., and Rahman, Z.: Assessment
1032 and characterization of particulate matter during the winter season in the urban
1033 environment of Lahore, Pakistan, Int. J. Environ. Sci. Technol., 21, 833–844,
1034 https://doi.org/10.1007/s13762-023-05011-7, 2024.

1035 Khodeir, M., Shamy, M., Alghamdi, M., Zhong, M., Sun, H., Costa, M., Chen, L.-C., and
1036 Maciejczyk, P.: Source apportionment and elemental composition of PM2.5 and PM10

https://doi.org/10.5194/egusphere-2026-6556
Preprint. Discussion started: 16 November 2026
© Author(s) 2026. CC BY 4.0 License.

in Jeddah City, Saudi Arabia, Atmos. Pollut. Res., 3, 331–340, https://doi.org/10.5094/apr.2012.037, 2012.

Kim Oanh, N. T., Upadhyay, N., Zhuang, Y. H., Hao, Z. P., Murthy, D. V. S., Lestari, P., Villarin, J. T., Chengchua, K., Co, H. X., Dung, N. T., and Lindgren, E. S.: Particulate air pollution in six Asian cities: spatial and temporal distributions, and associated sources, Atmos. Environ., 40, 3367–3380, https://doi.org/10.1016/j.atmosenv.2006.01.050, 2006.

Kolawole, T. O., Fomba, K. W., Ezeh, G. C., Olatunji, A. S., Ghazal, K. A., Mothes, F., and Herrmann, H.: Chemical composition, sources, and health risks assessment of PM10 and PM2.5-bound metals at an industrial site in Nigeria, Environ. Sci.: Atmos., 6, 104, https://doi.org/10.1039/d5ea00045a, 2026.

Kumar, S., Saha, N., Mohana, A. A., Hasan, M. S., Rahman, M. S., Elmes, M., and MacFarlane, G. R.: Atmospheric particulate matter and associated trace elements pollution in Bangladesh: a comparative study with global megacities, Water Air Soil Poll., 235, 222, https://doi.org/10.1007/s11270-024-07021-8, 2024.

Kusumaningtyas, S. D. A., Aldrian, E., Wati, T., Atmoko, D., and Sunaryo: The recent state of ambient air quality in Jakarta, Aerosol Air Qual. Res., 18, 2343–2354, https://doi.org/10.4209/aaqr.2017.10.0396, 2018.

Latif, M. T., Anuwar, N. Y. M., Srithawirat, T., Razak, I. S., and Ramli, N. A.: Composition of levoglucosan and surfactants in atmospheric aerosols from biomass burning, Aerosol Air Qual. Res., 11, 837–845, https://doi.org/10.4209/aaqr.2010.12.0103, 2011.

Lee, D. D. and Seung, H. S.: Learning the parts of objects by nonnegative matrix factorization, Nature, 401, 788–791, https://doi.org/10.1038/44565, 1999.

Li, J., Wang, G., Aggarwal, S. G., Huang, Y., Ren, Y., Zhou, B., Singh, K., Gupta, P. K., Cao, J., and Zhang, R.: Comparison of abundances, compositions and sources of elements, inorganic ions and organic compounds in atmospheric aerosols from Xi'an and New Delhi, two megacities in China and India, Sci. Total Environ., 476–477, 485–495, https://doi.org/10.1016/j.scitotenv.2014.01.011, 2014.

Li, J., Wang, G., Zhou, B., Cheng, C., Cao, J., Shen, Z., and An, Z.: Airborne particulate organics at the summit (2060 m, a.s.l.) of Mt. Hua in central China during winter: implications for biofuel and coal combustion, Atmos. Res., 106, 108–119, https://doi.org/10.1016/j.atmosres.2011.11.012, 2012.

Li, W., Ge, P., Chen, M., Tang, J., Cao, M., Cui, Y., Hu, K., and Nie, D.: Tracers from biomass burning emissions and identification of biomass burning, Atmosphere, 12, 1401, https://doi.org/10.3390/atmos12111401, 2021.

Li, X., Chen, M., Le, H. P., Wang, F., Guo, Z., Iinuma, Y., Chen, J., and Herrmann, H.: Atmospheric outflow of PM2.5 saccharides from megacity Shanghai to East China Sea: impact of biological and biomass burning sources, Atmos. Environ., 143, 1–14, https://doi.org/10.1016/j.atmosenv.2016.08.039, 2016a.

https://doi.org/10.5194/egusphere-2026-6556
Preprint. Discussion started: 16 November 2026
© Author(s) 2026. CC BY 4.0 License.

Li, X., Jiang, L., Le, P. H., Lyu, Y., Xu, T., Yang, X., Iinuma, Y., Chen, J., and Herrmann, H.: Size distribution of particle-phase sugar and nitrophenol tracers during severe urban haze episodes in Shanghai, Atmos. Environ., 145, 115–127, https://doi.org/10.1016/j.atmosenv.2016.09.030, 2016b.

Liang, L., Engling, G., Du, Z., Cheng, Y., Duan, F., Liu, X., and He, K.: Seasonal variations and source estimation of saccharides in atmospheric particulate matter in Beijing, China, Chemosphere, 150, 365–377, https://doi.org/10.1016/j.chemosphere.2016.02.002, 2016.

Liang, L., Han, Z., Li, J., and Liang, M.: Investigation of the influence of mineral dust on airborne particulate matter during the COVID-19 epidemic in spring 2020 over China, Atmos. Pollut. Res., 13, 101424, https://doi.org/10.1016/j.apr.2022.101424, 2022.

Lin, H., Liu, T., Xiao, J., Zeng, W., Li, X., Guo, L., Zhang, Y., Xu, Y., Tao, J., Xian, H., Syberg, K. M., Qian, Z., and Ma, W.: Mortality burden of ambient fine particulate air pollution in six Chinese cities: results from the Pearl River Delta study, *Environ. Int.*, 96, 91–97, https://doi.org/10.1016/j.envint.2016.09.007, 2016.

Louchouarn, P., Kuo, L. J., Wade, T. L., and Schantz, M. M.: Determination of levoglucosan and its isomers in size fractions of aerosol standard reference materials, Atmos. Environ., 43, 5630–5636, https://doi.org/10.1016/j.atmosenv.2009.07.040, 2009.

Lurie, K., Nayebare, S. R., Fatmi, Z., Carpenter, D. O., Siddique, A., Malashock, D., Khan, K., Zeb, J., Hussain, M. M., Khatib, F., and Khwaja, H. A.: PM2.5 in a megacity of Asia (Karachi): source apportionment and health effects, Atmos. Environ., 202, 223–233, https://doi.org/10.1016/j.atmosenv.2019.01.008, 2019.

Ma, S. X., Wang, Z. Z., Bi, X. H., Sheng, G. Y., and Fu, J. M.: Composition and source of saccharides in aerosols in Guangzhou, China, Chin. Sci. Bull., 54, 4500–4506, https://doi.org/10.1007/s11434-009-0287-z, 2009.

Ma, T., Duan, F., He, K., Qin, Y., Tong, D., Geng, G., Liu, X., Li, H., Yang, S., Ye, S., Xu, B., Zhang, Q., and Ma, Y.: Air pollution characteristics and their relationship with emissions and meteorology in the Yangtze River Delta region during 2014–2016, J. Environ. Sci., 83, 8–20, https://doi.org/10.1016/j.jes.2019.02.031, 2019.

Majumder, A. K., Mahmud, K. K., Rahman, M., Patoary, M. N. A., Gautam, S., and Tanima, K. R.: Spatial distribution and health implications of particulate matter concentrations across diverse land use types in Dinajpur District, Bangladesh, Geosyst. Geoenviron., 4, 100397, https://doi.org/10.1016/j.geogeo.2025.100397, 2025.

Manojkumar, N. and Srimuruganandam, B.: Size-segregated particulate matter and health effects in air pollution in India: a review, Environ. Chem. Lett., 19, 3837–3858, https://doi.org/10.1007/s10311-021-01277-w, 2021.

Medeiros, P. M., Conte, M. H., Weber, J. C., and Simoneit, B. R. T.: Sugars as source indicators of biogenic organic carbon in aerosols collected above the Howland Experimental Forest, Maine, Atmos. Environ., 40, 1694–1705, https://doi.org/10.1016/j.atmosenv.2005.11.001, 2006.

https://doi.org/10.5194/egusphere-2026-6556
Preprint. Discussion started: 16 November 2026
© Author(s) 2026. CC BY 4.0 License.

Michalski, R. and Kończyk, J.: Ion chromatography and related techniques in carbohydrate analysis: a review, Molecules, 29, 3413, https://doi.org/10.3390/molecules29143413, 2024.

Murari, V., Singh, N., Ranjan, R., Singh, R.S. and Banerjee, T.: Source apportionment and health risk assessment of airborne particulates over central Indo-Gangetic Plain, Chemosphere, 257, 127145, https://doi.org/10.1016/j.chemosphere.2020.127145, 2020.

Nadali, A., Arfaeinia, H., Asadgol, Z., and Fahiminia, M.: Indoor and outdoor concentration of PM10, PM2.5 and PM1 in residential building and evaluation of negative air ions (NAIs) in indoor PM removal, Environ. Pollut. Bioavailab., 32, 47–55, https://doi.org/10.1080/26395940.2020.1728198, 2020.

Nirmalkar, J., Deb, M. K., Deshmukh, D. K., Tsai, Y. I., and Verma, S. K.: Molecular markers in ambient aerosol in the Mahanadi Riverside Basin of eastern central India during winter, Environ. Sci. Pollut. R., 22, 1220–1231, https://doi.org/10.1007/s11356-014-3416-4, 2015b.

Nirmalkar, J., Deshmukh, D. K., Deb, M. K., Tsai, Y. I., and Sopajaree, K.: Mass loading and episodic variation of molecular markers in PM2.5 aerosols over a rural area in eastern central India, Atmos. Environ., 117, 41–50, https://doi.org/10.1016/j.atmosenv.2015.07.003, 2015a.

Omanga, E., Ulmer, L., Berhane, Z., and Gatari, M.: Industrial air pollution rural Kenya: community awareness, risk perception and associations between risk variables, BMC Public Health, 14, 377, https://doi.org/10.1186/1471-2458-14-377, 2014.

Othman, M., Latif, M. T., Hamid, H. H. A., Uning, R., Khumsaeng, T., Phairuang, W., Daud, Z., Idris, J., Sofwan, N. M., and Lung, S.-C. C.: Spatial–temporal variability and health impact of particulate matter during a 2019–2020 biomass burning event in Southeast Asia, Sci. Rep., 12, 7630, https://doi.org/10.1038/s41598-022-11409-z, 2022.

Pabel, M. Y., Islam, M. F., Huda, M. N., Hossain, S. A., Rahman, M. M., and Islam, M. M.: Formation of particulate matter in the ambient air of Dhaka city, Bangladesh, Air Qual. Atmos. Health, 18, 239–251, https://doi.org/10.1007/s11869-024-01642-y, 2025.

Pakbin, P., Hudda, N., Cheung, K. L., Moore, K. F., and Sioutas, C.: Spatial and temporal variability of coarse (PM10−2.5) particulate matter concentrations in the Los Angeles area, Aerosol Sci. Tech., 44, 514–525, https://doi.org/10.1080/02786821003749509, 2010.

Pakistan Bureau of Statistics: 7th Population & Housing Census 2023: National census report (first ever digital census), Ministry of Planning Development and Special Initiatives, Government of Pakistan, Islamabad, https://www.pbs.gov.pk (last access: 30 September 2026), 2024.

Pakistan Environmental Protection Agency: The health effects of air pollution on school children in Murree, Pak-EPA, Government of Pakistan, 15 pp., https://web.archive.org/web/20081209012850/http://www.environment.gov.pk/Publications.htm (last access: 30 September 2026), 2006.

https://doi.org/10.5194/egusphere-2026-6556
Preprint. Discussion started: 16 November 2026
© Author(s) 2026. CC BY 4.0 License.

Panda, S. and Nagendra, S. S.: Chemical and morphological characterization of respirable suspended particulate matter (PM10) and associated health risk at a critically polluted industrial cluster, Atmos. Pollut. Res., 9, 791–803, https://doi.org/10.1016/j.apr.2018.01.011, 2018.

Pardo, M., Offer, S., Hartner, E., Di Bucchianico, S., Bisig, C., Bauer, S., Pantzke, J., Zimmermann, E. J., Cao, X., Binder, S., and Kuhn, E.: Exposure to naphthalene and β-pinene-derived secondary organic aerosol induced divergent changes in transcript levels of BEAS-2B cells, Environ. Int., 166, 107366, https://doi.org/10.1016/j.envint.2022.107366, 2022.

Paris, E., Carnevale, M., Guerriero, E., Palma, A., Vincenti, B., Khalid, A., Rantica, E., Proto, A. R., and Gallucci, F.: Fixed source monitoring system for marker emission during biomass combustion, Renew. Energy, 208, 597–603, https://doi.org/10.1016/j.renene.2023.03.116, 2023.

Paris, E., Carnevale, M., Palma, A., Vincenti, B., Salerno, M., Proto, A. R., Papandrea, S., Guerriero, E., Perilli, M., Cerasa, M., Di Stefano, V., and Gallucci, F.: Biomass combustion in boiler: environmental monitoring of sugar markers and pollutants, Atmosphere, 15, 427, https://doi.org/10.3390/atmos15040427, 2024.

Pietrogrande, M. C., Bacco, D., Visentin, M., Ferrari, S., and Casali, P.: Polar organic marker compounds in atmospheric aerosol in the Po Valley during the Supersito campaigns – Part 2: Seasonal variations of sugars, Atmos. Environ., 97, 215–225, https://doi.org/10.1016/j.atmosenv.2014.07.056, 2014.

Pope, C. A., III and Dockery, D. W.: Health effects of fine particulate air pollution: lines that connect, J. Air Waste Manage. Assoc., 56, 709–742, https://doi.org/10.1080/10473289.2006.10464485, 2006.

Pradhan, D. S., Patra, A. K., Santra, S., Penchala, A., Sahu, S. P., and Nazneen: In-cabin particulate matter exposure of heavy earth moving machinery operators in Indian opencast coal mine, Aerosol Sci. Eng., 9, 259–276, https://doi.org/10.1007/s41810-024-00258-0, 2025.

Punjab Board of Investment and Trade: Investment opportunities and sectoral profile of Punjab, Government of the Punjab, Lahore, Pakistan, https://pbit.gop.pk/sectoral-briefs?page=0 (last access: 30 September 2026), 2024.

Rabhi, L., Lemou, A., Ladji, R., Khedidji, S., Bonnaire, N., Sciare, J., and Yassaa, N.: Size distribution of water-soluble ions and carbon content in the Southwest Mediterranean Basin, Air Qual. Atmos. Health, 17, 1530, https://doi.org/10.1007/s11869-024-01614-2, 2024.

Rabhi, L., Lemou, A., Ladji, R., Khedidji, S., Bonnaire, N., Sciare, J., and Yassaa, N.: Size-distribution of particulate saccharides at a coastal site in the South Western Mediterranean: sources and formation processes, Int. J. Environ. Sci. Technol., 22, 16687–16704, https://doi.org/10.1007/s13762-025-06726-5, 2025.

https://doi.org/10.5194/egusphere-2026-6556
Preprint. Discussion started: 16 November 2026
© Author(s) 2026. CC BY 4.0 License.

Rahman, M. H., Sharma, V. P., Kundu, S., and Datta, A.: Seasonal variation of potential source locations of atmospheric particulates over the Indo-Gangetic Plain of India, Open J. Air Pollut., 9, 1–17, https://doi.org/10.4236/ojap.2020.91001, 2020.

Rajput, P., Izhar, S., and Gupta, T.: Deposition modeling of ambient aerosols in human respiratory system: health implication of fine particles penetration into the pulmonary region, Atmos. Pollut. Res., 10, 334–343, https://doi.org/10.1016/j.apr.2018.08.013, 2019.

Rajput, P., Sarin, M. M., Rengarajan, R., and Singh, D.: Atmospheric polycyclic aromatic hydrocarbons (PAHs) from post-harvest biomass burning emissions in the Indo-Gangetic Plain: isomer ratios and temporal trends, Atmos. Environ., 45, 6732–6740, https://doi.org/10.1016/j.atmosenv.2011.08.018, 2011.

Rajput, P., Sarin, M., Sharma, D., and Singh, D.: Characteristics and emission budget of carbonaceous species from post-harvest agricultural-waste burning in source region of the Indo-Gangetic Plain, Tellus B, 66, 21026, https://doi.org/10.3402/tellusb.v66.21026, 2014.

Ramteke, S., Sahu, B. L., Patel, K. S., Pandey, P. K., Yurdakul, S., Martín-Ramos, P., Ren, H., and Fu, P.: Characterization of organic aerosols in the ambient air of Raipur, Central India: distribution, seasonal variations, and source apportionment, Aerosol Sci. Eng., 9, 89–103, https://doi.org/10.1007/s41810-024-00246-4, 2025.

Ramteke, S., Sahu, B. L., Savita, S., Mondal, B., Patel, K. S., Ren, H., and Fu, P.: Size-segregation and distribution of organic aerosol in different industrial areas of Raipur region, J. Geointerface, 1, 103–126, https://cehesh.in/contents/july2022vol1/13.Dr.B.L.Sahu %20p.103-125.pdf, 2022.

Rehman, A., Liu, G., Yousaf, B., Ijaz, S., Irshad, S., Cheema, A. I., Riaz, M. U., and Ashraf, A.: Spectroscopic fingerprinting, pollution characterization, and health risk assessment of potentially toxic metals from urban particulate matter, Environ. Sci. Pollut. R., 30, 92842–92858, https://doi.org/10.1007/s11356-023-28834-w, 2023.

Rengarajan, R., Sudheer, A. K., and Sarin, M. M.: Wintertime PM2.5 and PM10 carbonaceous and inorganic constituents from urban site in western India, Atmos. Res., 102, 420–431, https://doi.org/10.1016/j.atmosres.2011.09.005, 2011.

Saikawa, E., Panday, A., Kang, S., Gautam, R., Zusman, E., Cong, Z., Somanathan, E., and Adhikary, B.: Air pollution in the Hindu Kush Himalaya, in: The Hindu Kush Himalaya Assessment, edited by: Wester, P., Mishra, A., Mukherji, A., and Shrestha, A. B., Springer, Cham, 339–387, https://doi.org/10.1007/978-3-319-92288-1_10, 2019.

Saju, J. A., Bari, Q. H., Mohiuddin, K. A. B. M., and Strezov, V.: Measurement of ambient particulate matter (PM1.0, PM2.5 and PM10) in Khulna City of Bangladesh and their implications for human health, Environ. Syst. Res., 12, 42, https://doi.org/10.1186/s40068-023-00327-2, 2023.

https://doi.org/10.5194/egusphere-2026-6556
Preprint. Discussion started: 16 November 2026
© Author(s) 2026. CC BY 4.0 License.

Sang-Arlt, X., Fu, H., Zhang, Y., Ding, X., Wang, X., Zhou, Y., Zou, L., Zellmer, G. F., and Engling, G.: Carbonaceous aerosol emitted from biofuel household stove combustion in South China, Atmosphere, 11, 112, https://doi.org/10.3390/atmos11010112, 2020.

Scaramboni, C., Urban, R. C., Lima-Souza, M., Nogueira, R. F. P., Cardoso, A. A., Allen, A. G., and Campos, M. L. A. M.: Total sugars in atmospheric aerosols: an alternative tracer for biomass burning, Atmospheric Environment, 100, 185–192, https://doi.org/10.1016/j.atmosenv.2014.11.003, 2015.

Shah, M. H., Shaheen, N., and Nazir, R.: Assessment of the trace elements level in urban atmospheric particulate matter and source apportionment in Islamabad, Pakistan, Atmos. Pollut. Res., 3, 39–45, https://doi.org/10.5094/APR.2012.003, 2012.

Shahid, M. Z., Liao, H., Li, J., Shahid, I., Lodhi, A., and Mansha, M.: Seasonal variations of aerosols in Pakistan: contributions of domestic anthropogenic emissions and transboundary transport, Aerosol Air Qual. Res., 15, 1580–1600, https://doi.org/10.4209/aaqr.2014.12.0332, 2015.

Shahid, M. Z., Shahzad, M. I., Jaweria, S., Javed, S., Zaib, S., and Shahid, I.: Characteristics of aerosols and planetary boundary layer dynamics during biomass burning season, Nat. Hazards, 121, 12531–12549, https://doi.org/10.1007/s11069-025-07295-z, 2025.

Shahzad, M. I., Khalid, S., Khalid, S., Iqbal, N., Rasheed, A., and Raza, G.: Estimating surface visibility at Hong Kong from ground-based LIDAR, J. Air Waste Manage. Assoc., 63, 1098–1110, https://doi.org/10.1080/10962247.2013.801372, 2013.

Shahzadi, H. K., Sultan, K., Sultan, J., Zaman, Q. U., Nazir, A., Mnif, W., Iqbal, S., Ahmad, N., and Iqbal, M.: Assessing the spatial and temporal dynamics of specific airborne pollutants in industrial and agricultural ecosystems, Ecol. Front., 44, 802–808, https://doi.org/10.1016/j.ecofro.2024.04.001, 2024.

Shang, X., Zhang, K., Meng, F., Wang, S., Lee, M., Suh, I., Kim, D., Jeon, K., Park, H., Wang, X., and Zhao, Y.: Characteristics and source apportionment of fine haze aerosol in Beijing during the winter of 2013, Atmos. Chem. Phys., 18, 2573–2584, https://doi.org/10.5194/acp-18-2573-2018, 2018.

Shao, P., Gao, Y., Zhang, X., Zhang, T., Zhou, J., Tian, R., Ye, Z., Wei, C., and Zhao, Z.: Assessing biogenic and biomass burning sources in winter PM2.5 through saccharide characterization in Changzhou, YRD region, China, Aerosol Sci. Eng., 10, 1–14, https://doi.org/10.1007/s41810-026-00408-6, 2026.

Sharma, M., Kaskaoutis, D. G., Singh, R. P., and Singh, S.: Seasonal variability of atmospheric aerosol parameters over Greater Noida using ground sunphotometer observations, Aerosol Air Qual. Res., 14, 608–622, https://doi.org/10.4209/aaqr.2013.06.0219, 2014.

Simoneit, B. R. T., Elias, V. O., Kobayashi, M., Kawamura, K., Rushdi, A. I., Medeiros, P. M., Rogge, W. F., and Didyk, B. M.: Sugars-dominant water-soluble organic compounds in soils and characterization as tracers in atmospheric particulate matter, Environ. Sci. Technol., 38, 5939–5949, https://doi.org/10.1021/es0403099, 2004.

https://doi.org/10.5194/egusphere-2026-6556
Preprint. Discussion started: 16 November 2026
© Author(s) 2026. CC BY 4.0 License.

Simoneit, B. R. T., Schauer, J. J., Nolte, C. G., Oros, D. R., Elias, V. O., Fraser, M. P., Rogge, W. F., and Cass, G. R.: Levoglucosan, a tracer for cellulose in biomass burning and atmospheric particles, Atmos. Environ., 33, 173–182, https://doi.org/10.1016/S1352-2310(98)00145-9, 1999.

Singh, A. K., Pathak, A. K., and Saini, G.: Respiratory deposition dose and associated health risks of particulate matter (PM2.5 and PM10) in Delhi, India, Sci. Rep., 15, 26663, https://doi.org/10.1038/s41598-025-26663-0, 2025.

Skiba, A., Styszko, K., Tobler, A., Casotto, R., Gorczyca, Z., Furman, P., Samek, L., Wideł, D., Zimnoch, M., Kasper-Giebl, A., Slowik, J. G., Daellenbach, K. R., Prévôt, A. S. H., and Różański, K.: Source attribution of carbonaceous fraction of particulate matter in the urban atmosphere based on chemical and carbon isotope composition, Sci. Rep., 14, 7308, https://doi.org/10.1038/s41598-024-57829-x, 2024.

Son, J., Jeong, S., Park, H., and Park, C. E.: The effect of particulate matter on solar photovoltaic power generation over the Republic of Korea, Environ. Res. Lett., 15, 084004, https://doi.org/10.1088/1748-9326/ab905b, 2020.

Sowmya, V., Shiva Nagendra, S. M., and Gulia, S.: Spatiotemporal distribution and source apportionment of fine particulate matter in urban microenvironments, Air Qual. Atmos. Health, 17, 815–829, https://doi.org/10.1007/s11869-023-01490-2, 2024.

Stone, E., Schauer, J., Quraishi, T. A., and Mahmood, A.: Chemical characterization and source apportionment of fine and coarse particulate matter in Lahore, Pakistan, Atmos. Environ., 44, 1062–1070, https://doi.org/10.1016/j.atmosenv.2009.12.015, 2010.

Suciu, L. G., Masiello, C. A., and Griffin, R. J.: Anhydrosugars as tracers in the Earth system, Biogeochemistry, 146, 209–256, https://doi.org/10.1007/s10533-019-00622-0, 2019.

Supasri, T., Gheewala, S. H., Macatangay, R., Chakpor, A., and Sedpho, S.: Association between ambient air particulate matter and human health impacts in northern Thailand, Sci. Rep., 13, 12753, https://doi.org/10.1038/s41598-023-39930-9, 2023.

Tabinda, A. B., Anjum, Z., Yasar, A., Rasheed, R., Mahmood, A., and Iqbal, A.: Determination and dispersion of pollutants from different fuel types used in brick kilns by using Gaussian's plume model, Energ. Source. Part A, 41, 1022–1028, https://doi.org/10.1080/15567036.2018.1539135, 2019.

Theodosi, C., Panagiotopoulos, C., Nouara, A., Panagiotis, Z., Maria, K., and Nikos, M.: Sugars in atmospheric aerosols over the Eastern Mediterranean, Prog. Oceanogr., 163, 70–81, https://doi.org/10.1016/j.pocean.2017.09.001, 2018.

Tsai, Y. I., Wu, P. L., Hsu, Y. T., and Yang, C. R.: Anhydrosugar and sugar alcohol organic markers associated with carboxylic acids in particulate matter from incense burning, Atmos. Environ., 44, 3708–3718, https://doi.org/10.1016/j.atmosenv.2010.06.030, 2010.

Valavanidis, A., Fiotakis, K., and Vlachogianni, T.: Airborne particulate matter and human health: toxicological assessment and importance of size and composition of particles for

https://doi.org/10.5194/egusphere-2026-6556
Preprint. Discussion started: 16 November 2026
© Author(s) 2026. CC BY 4.0 License.

oxidative damage and carcinogenic mechanisms, J. Environ. Sci. Health C, 26, 339–362, https://doi.org/10.1080/10590500802494538, 2008.

Vincenti, B., Paris, E., Carnevale, M., Palma, A., Guerriero, E., Borello, D., Paolini, V., and Gallucci, F.: Saccharides as particulate matter tracers of biomass burning: a review, Int. J. Environ. Res. Public Health, 19, 4387, https://doi.org/10.3390/ijerph19074387, 2022.

Waheed, S., Rahman, A., Khalid, N., and Ahmad, S.: Assessment of air quality of two metropolitan cities in Pakistan: elemental analysis using INAA and AAS, Radiochim. Acta, 94, 161–166, https://doi.org/10.1524/ract.2006.94.3.161, 2006.

Wang, G. H., Kawamura, K., Lee, S. C., Ho, K. F., and Cao, J. J.: Molecular, seasonal, and spatial distributions of organic aerosols from fourteen Chinese cities, Environ. Sci. Technol., 40, 4619–4625, https://doi.org/10.1021/es060291x, 2006a.

Wang, G., Chen, C., Li, J., Zhou, B., Xie, M., Hu, S., Kawamura, K., and Chen, Y.: Molecular composition and size distribution of sugars, sugar-alcohols and carboxylic acids in airborne particles during a severe urban haze event caused by wheat straw burning, Atmos. Environ., 45, 2473–2479, https://doi.org/10.1016/j.atmosenv.2011.02.045, 2011.

Wang, G., Kawamura, K., Hatakeyama, S., Takami, A., Li, H., and Wang, W.: Aircraft measurement of organic aerosols over China, Environ. Sci. Technol., 41, 3115–3120, https://doi.org/10.1021/es062601h, 2007.

Wang, X., Bi, X., Sheng, G., and Fu, J.: Chemical composition and sources of PM10 and PM2.5 aerosols in Guangzhou, China, Environ. Monit. Assess., 119, 425–439, https://doi.org/10.1007/s10661-005-9034-3, 2006b.

Wang, Z., Wu, D., Li, Z., Shang, X., Li, Q., Li, X., Chen, R., Kan, H., Ouyang, H., Tang, X., and Chen, J.: Measurement report: Saccharide composition in atmospheric fine particulate matter during spring at the remote sites of southwest China and estimates of source contributions, Atmos. Chem. Phys., 21, 12227–12241, https://doi.org/10.5194/acp-21-12227-2021, 2021.

Wen, T.-Y., Chantara, S., Jalaludin, J., Lestari, P., Syafei, A. D., Pham, T. V., and Tsai, Y. I.: Overview of aerosol and air pollution in South Eastern Asia countries, Aerosol Air Qual. Res., 23, 230055, https://doi.org/10.4209/aaqr.230055, 2023.

Werden, B. S., Giordano, M. R., Mahata, K., Islam, M. R., Goetz, J. D., Puppala, S. P., Saikawa, E., Panday, A. K., Yokelson, R. J., Stone, E. A., and DeCarlo, P. F.: Submicron aerosol composition and source contribution across the Kathmandu Valley, Nepal, in winter, ACS Earth Space Chem., 7, 49–68, https://doi.org/10.1021/acsearthspacechem.2c00226, 2023.

World Health Organization: WHO global ambient air quality database (update 2018), World Health Organization, Geneva, https://www.who.int/data/gho/data/themes/air-pollution/who-air-quality-database/2018 (last access: 30 September 2026), 2018.

https://doi.org/10.5194/egusphere-2026-6556
Preprint. Discussion started: 16 November 2026
© Author(s) 2026. CC BY 4.0 License.

Xie, M., Wang, G., Hu, S., Gao, S., Han, Q., Xu, Y., and Feng, J.: Polar organic and inorganic markers in PM10 aerosols from an inland city of China – seasonal trends and sources, Sci. Total Environ., 408, 5452–5460, https://doi.org/10.1016/j.scitotenv.2010.07.029, 2010.

Xie, Y. L., Hopke, P. K., Paatero, P., Barrie, L. A., and Li, S. M.: Identification of source nature and seasonal variations of Arctic aerosol by positive matrix factorization, J. Atmos. Sci., 56, 249–260, https://doi.org/10.1175/1520-0469(1999)056<0249:IOSNAS>2.0.CO;2, 1999.

Yadav, S., Praveen, O. D., and Satsangi, P. G.: The effect of climate and meteorological changes on particulate matter in Pune, India, Environ. Monit. Assess., 187, 402, https://doi.org/10.1007/s10661-015-4634-z, 2015.

Yang, F., Kawamura, K., Chen, J., Ho, K., Lee, S., Gao, Y., Cui, L., Wang, T., and Fu, P.: Anthropogenic and biogenic organic compounds in summertime fine aerosols (PM2.5) in Beijing, China, Atmos. Environ., 124, 166–175, https://doi.org/10.1016/j.atmosenv.2015.08.095, 2016.

Yttri, K. E., Dye, C., and Kiss, G.: Ambient aerosol concentrations of sugars and sugar-alcohols at four different sites in Norway, Atmos. Chem. Phys., 7, 4267–4279, https://doi.org/10.5194/acp-7-4267-2007, 2007.

Yunesian, M., Hasanvand, M. S., and Fotouhi, A.: Exposure to ambient air pollution and risk of childhood cancers: a population-based case-control study in Tehran, Iran, Sci. Total Environ., 646, 105–110, https://doi.org/10.1016/j.scitotenv.2018.07.219, 2019.

Zeb, B. B., Alam, K., Sorooshian, A. A., Blaschke, T., Ahmad, I., and Shahid, I.: On the morphology and composition of particulate matter in an urban environment, Aerosol Air Qual. Res., 18, 1431–1447, https://doi.org/10.4209/aaqr.2017.09.0340, 2018.

Zeb, B., Alam, K., Ditta, A., Ullah, S., Ali, H. M., Ibrahim, M., and Salem, M. Z. M.: Variation in coarse particulate matter (PM10) and its characterization at multiple locations in the semiarid region, Front. Environ. Sci., 10, 843582, https://doi.org/10.3389/fenvs.2022.843582, 2022.

Zhai, S., Jacob, D. J., Pendergrass, D. C., Colombi, N. K., Shah, V., Yang, L. H., Zhang, Q., Wang, S., Kim, H., Sun, Y., Choi, J.-S., Park, J.-S., Luo, G., Yu, F., Woo, J.-H., Kim, Y., Dibb, J. E., Lee, T., Han, J.-S., Anderson, B. E., Li, K., and Liao, H.: Coarse particulate matter air quality in East Asia: implications for fine particulate nitrate, Atmos. Chem. Phys., 23, 4271–4281, https://doi.org/10.5194/acp-23-4271-2023, 2023.

Zhang, K., Shang, X. N., Herrmann, H., Meng, F., Mo, Z. Y., Chen, J. H., and Lv, M. L.: Approaches for identifying PM2.5 source types and source areas at a remote background site of South China in spring, Sci. Total Environ., 691, 1320–1327, https://doi.org/10.1016/j.scitotenv.2019.07.178, 2019.

Zhang, L., Liu, T., Zhang, J., Zhu, B., Xiang, D., Zhao, X., and Liu, X.: Bioaerosol seasonal variation and contribution to airborne particulate matter in Huangshi city of Central China, Atmosphere, 13, 909, https://doi.org/10.3390/atmos13060909, 2022.

https://doi.org/10.5194/egusphere-2026-6556
Preprint. Discussion started: 16 November 2026
© Author(s) 2026. CC BY 4.0 License.



Zhang, Q., Qiu, Z., Chung, K. F., and Huang, S. K.: Link between environmental air pollution and allergic asthma: East meets West, J. Thorac. Dis., 7, 14–22, https://doi.org/10.3978/j.issn.2072-1439.2014.12.07, 2015.

Zhang, T., Claeys, M., Cachier, H., Dong, S. P., Wan, W., Maenhaut, W., and Liu, X. D.: Identification and estimation of the biomass burning contribution to Beijing aerosol using levoglucosan as a molecular marker, Atmos. Environ., 42, 7013–7021, https://doi.org/10.1016/j.atmosenv.2008.04.050, 2008a.

Zhang, Y., Quraishi, T., and Schauer, J. J.: Daily variations in sources of carbonaceous aerosol in Lahore, Pakistan during a high pollution spring episode, Aerosol Air Qual. Res., 8, 130–146, https://doi.org/10.4209/aaqr.2007.09.0042, 2008b.